

Locally Localized Gravity: The Inside Story

Nemanja Kaloper

Department of Physics, University of California, Davis, CA 95616, USA

and

IHES, 35 Route de Chartres, F-91440 Bures-sur-Yvette, France

E-mail: kaloper@physics.ucdavis.edu

Lorenzo Sorbo

Department of Physics, University of California, Davis, CA 95616, USA

E-mail: sorbo@physics.ucdavis.edu

ABSTRACT: We derive the exact gravitational field of a relativistic particle localized on an AdS 3-brane, with curvature radius ℓ , in AdS_5 bulk with radius L . The solution is a gravitational shock wave. We use it to explore the dynamics of locally localized tensor gravitons over a wide range of scales. At distances below L the shock wave looks exactly like the $5D$ GR solution. Beyond L the solution approximates very closely the shock wave in $4D$ AdS space all the way out to distances ℓ^3/L^2 along the brane. At distances between L and ℓ , the effective $4D$ graviton is a composite built of the ultralight mode and heavier gravitons, whereas between ℓ and ℓ^3/L^2 it is just the ultralight mode. Finally beyond ℓ^3/L^2 the shock reveals a glimpse of the fifth dimension, since the ultralight mode wave function decays to zero at the rate inherited from the full $5D$ geometry. We obtain the precise bulk-side formula for the $4D$ Planck mass, defined as the coupling of the ultralight mode, in terms of the $5D$ Planck mass and the curvature radii. It includes higher-order corrections in L/ℓ , and reduces to the RS2 formula in the limit $\ell \rightarrow \infty$. We discuss AdS/CFT interpretation of these results, and argue that the spatial variation of the effective gravitational coupling read from the shock wave amplitude corresponds to RG running driven by quantum effects in the dual CFT .

KEYWORDS: Localization of Gravity, AdS/CFT, Braneworlds.

Contents

1. Introduction	1
1.1 Prelude	1
1.2 Summary of the Main Results	3
2. Setup	6
3. Shocks	9
4. Limits	11
4.1 Surfing the Wave	12
4.1.1 Spectral Decomposition of the Shock Wave	13
4.1.2 Short Distance Behavior	16
4.1.3 Composite Graviton Regime	17
4.1.4 Ultralight Graviton Dominance	19
4.1.5 A Peek into AdS_5	21
4.2 Recovering Minkowski	22
5. Conclusions	24
A. Derivation of the Wave Profile Field Equation	27
B. Series Representation of the Shock Wave	29
C. Spectrum of $AdS_4 \subset AdS_5$: Masses and Couplings	30
D. The Limit of RS2 Shock Wave	32

1. Introduction

1.1 Prelude

The models of localized gravity in AdS space [1] offer a new possibility for deriving $4D$ gravity at large distances from a higher dimensional theory. Unlike in the conventional

Kaluza-Klein (KK) approach, the extra dimensions could be infinite [1, 2, 3]. However, when the boundary brane is Minkowski [1, 2, 3] or de Sitter [3, 4], the bulk volume is still finite. This yields a normalizable $4D$ zero mode graviton, whose dynamics is described by $4D$ General Relativity (GR). In addition, one also finds a continuum of massive KK modes. It comes about because the boundary conditions far in the bulk are arbitrary, and so the boundary value problem is one-sided. In a certain sense these models might be thought of as “semi-compactifications”. Despite the KK continuum, gravity below the cutoff appears $4D$ all the way down to infinity. This is because the light KK modes couple to the brane probes exponentially weakly, since they must climb the bulk gravitational well to get to the brane, which in perturbation theory appears as the familiar volcano potential suppression of [1]. This theory admits AdS/CFT interpretation as a dual CFT with a cutoff coupled to $4D$ gravity [5, 6].

On the other hand, in the case of an AdS_4 3-brane embedded in AdS_5 , or $AdS_4 \subset AdS_5$ for short, the bulk volume is infinite [4, 7]. The exact $4D$ zero mode graviton decouples since the scale which controls its coupling, set by the bulk volume, diverges. However, there arises a new light spin-2 mode with a mass $m \sim \ell^{-1} \arcsin(L/\ell)$, where L and ℓ are 5- and 4-dimensional AdS radii, respectively [8, 9]. It is normalizable, and when $\ell \gg L$, it is anomalously light, $m \sim L/\ell^2$, resembling the $4D$ zero mode graviton. It plays a key role in the locally localized gravity scenario advocated in [8, 10, 11]. However, it is not completely clear how to compute the $4D$ Planck mass M_4 in locally localized gravity. Numerical integration [8] of the ultralight mode wave function suggests that $M_4^2 \sim M_5^3 L$, qualitatively as in RS2 [1]. The arguments of [18] based on covariant entropy bound and light-like holography should yield a finite answer, relating M_4 in some way to M_5 and the finite volume of the brane’s holographic domain. However [18] do not give an explicit expression for this relation. Formulating $AdS_4 \subset AdS_5$ as a dual effective CFT coupled to AdS_4 gravity cut off at $1/L$, [19] computes the Planck scale to be¹ $M_4^2 = M_5^3 L$, precisely as in RS2 [1]. Yet in light of [18] one might be circumspect about using AdS/CFT picture in the far infra-red. The dual description based on the idea of defect CFT [20] offers a very nice picture, whereby a fat defect generates a small anomalous dimension of CFT operators that yield an ultralight graviton, but the calculations involve strong coupling dynamics and are not under complete control yet. Thus it is very interesting to find a more precise rule for the calculation of M_4 . It is also interesting to find out whether gravity changes form from $4D$ to $5D$, and where, if at all. In [8], it has been suggested that at distances $\gtrsim m^{-1} \sim \ell^2/L$, the AdS_4 curvature screens out the deviations from the $4D$ gravity law. In [18] it was further argued that gravity may remain $4D$ at all spatial scales for

¹This is the correct formula with normalizations as found in [1, 2].

experiments that do not last longer than a time $\Delta t \sim \ell$, but a more precise statement is still lacking. These issues are puzzling, and resolving them will shed more light on the mechanism of locally localized gravity.

1.2 Summary of the Main Results

In this work we are able to explicitly calculate, on the bulk side, the precise expressions for the $4D$ Planck scale M_4 and the IR length scale at which gravity starts feeling the fifth dimension. We derive the exact solution for the gravitational field of a relativistic particle on the brane, a “photon”, which generalizes the Aichelburg-Sexl shock wave of $4D$ GR [21, 22] to $AdS_4 \subset AdS_5$ braneworlds. This is the first example of an exact gravitational field of a particle in locally localized gravity. It includes contributions from all the tensor gravitons in the bulk spectrum, which contains three sectors: the ultralight graviton with mass $m \sim L/\ell^2$, a tower of “intermediate” gravitons with masses $m \sim n/\ell$, and the sector of “heavy” gravitons with masses $m > 1/L$ [8, 9]. The couplings of heavier gravitons are suppressed relative to the ultralight one by $\frac{L}{\ell}mL$, similar to RS2 [1, 23], eventually saturating at $\frac{1}{M_5^3\ell}$ for $m \gg L^{-1}$. We analyze the solution in the regime $1/M_5 \ll L \ll \ell$ in order to separate the scales that control the dynamics of the theory in a clear way. The intricacies of the spectrum result in the emergence of *four* interesting regimes of scales:

I: $\mathcal{R} \ll L$: At distances much shorter than the AdS_5 radius L , the solution looks $5D$ as dictated by the short distance singularities of the longitudinal Green’s function. Because the momentum transfer between the source of the gravitational field and a probe particle is so high ($> 1/L$) all the graviton modes contribute, and in particular the very heavy ones dominate since they outnumber the light modes and their couplings are less suppressed, and their Yukawa-suppressions are negligible in this regime.

II: $L < \mathcal{R} < \ell$: At a fixed distance \mathcal{R} within this range, the shock wave is *composite*: all intermediate gravitons with masses² $m < 2/\mathcal{R}$ contribute to it, but only at $\mathcal{O}(L^2/\ell^2)$ relative to the ultralight mode because of the coupling suppression. The solution approximates very closely the $4D$ Aichelburg-Sexl solution, $f_{A-S} \simeq \frac{p}{\pi} G_{eff} \log \frac{\mathcal{R}}{2\ell}$, where the logarithm gradually changes towards the AdS_4 shock wave as distance increases. Defining G_{eff} as the $4D$ effective gravitational coupling which controls the deflection imparted by the shock on a test particle as in $4D$ [24, 25], we note that it *runs*³. On the bulk side this is a completely

²The extra helicity states of massive gravitons which plague flat space perturbation theory [12] could be circumvented in curved backgrounds [13]. For discussions including the ghosts see [14, 15, 16, 17].

³We thank John Terning for related discussions about such phenomena.

classical effect. The intermediate gravitons drop out from the resonance as the distance increases due to Yukawa suppression; after each step $\sim \ell/n$ of distance, G_{eff} drops by $\frac{\Delta G_{eff}}{G_{eff}} \sim n \frac{L^2}{2\ell^2}$. These jumps are sharp, and are the largest at the shortest distances, never exceeding $L/\ell \ll 1$ in this regime. So overall gravity remains $4D$. Except for the coupling suppression of all heavier modes generated by warping, this regime resembles gravity on a space with a large compact dimension at distances between the cutoff and the compactification radius [26].

III: $\ell \lesssim \mathcal{R} < \ell^3/L^2$: All heavier gravitons are now decoupled, and the behavior of the shock wave at these distances is completely set by the ultralight mode, which mimics $4D$ gravity with great accuracy. To the leading order, the shock wave behaves as the AdS_4 shock, succumbing to the AdS_4 curvature. Although the heavier gravitons have decoupled, the small graviton mass feeds the weak running of the $4D$ effective gravitational coupling with distance. It yields subleading distance-dependent corrections to the shock, which appear as a multiplicative factor in the amplitude $\sim \left(1 - \mathcal{O}(1) \frac{L^2 \mathcal{R}}{\ell^2}\right)$, continuing to weaken gravity.

IV: $\ell^3/L^2 < \mathcal{R}$: At such large distances along the brane, the subleading corrections controlled by the mass of the ultralight graviton pick up. Due to the graviton mass, the gravitational force weakens faster. However these mass-induced corrections open a narrow window into the fifth dimension. The ultralight graviton mass probes the full $5D$ geometry, making the decay rate of the ultralight graviton wave function a little *slower* than it would have been if the decay rate were controlled by a perturbative graviton mass term in AdS_4 . Probing this regime one would discover both the graviton mass and the hidden extra dimension.

From the solution, we extract the formula for the $4D$ Planck mass in terms of the $5D$ Planck mass and the curvature radii, defined as the inverse coupling of the ultralight mode. It is⁴

$$M_4^2 = \frac{2M_5^3 \ell}{2\nu + 1} \frac{[-\partial_\nu P_\nu^{-1}(-\cos(y_0))]}{P_\nu^{-2}(-\cos(y_0))} \Big|_{\nu=\nu_0}, \quad (1.1)$$

where P_ν^k are Legendre functions, $y_0 = \arcsin(L/\ell)$, and $\nu_0 = [\sqrt{9 + 4\ell^2 m^2} - 1]/2$ where m is the ultralight mode mass. This reproduces exactly $M_4^2 = M_5^3 L$ to the leading order in $L/\ell \ll 1$, supporting the arguments of [19]. However, there are also higher order corrections in L/ℓ , showing that the dual CFT is modified in the far infra-red. This stems from AdS/CFT , which relates classical bulk dynamics with the dual CFT in the large N limit, including quantum corrections from planar diagrams [6].

⁴The $(-)$ sign cancels another $(-)$ sign hidden in $\partial_\nu P_\nu^{-1}$.

To recap, from the bulk view point low energy localized gravity is born from a conspiracy between the AdS_4 and AdS_5 curvatures. Together they give rise to the ultra-light mode. The brane curvature separates the rest of the spectrum from it by a mass gap $\sim \ell^{-1}$. In turn, the bulk curvature pulls all modes with masses $m \gtrsim 1/\ell$ away from the brane, suppressing their coupling relative to the ultralight mode by a power mL^2/ℓ , as in RS2 [1, 23]. Thus the shock wave appears $4D$ to the leading order even at distances $\mathcal{R} < \ell$, at which many intermediate gravitons contribute to it. Without the suppression of the couplings the running of G_{eff} would have been much faster, spoiling the $4D$ guise of the shock wave. At very large distances, $\mathcal{R} > \ell$, brane curvature kicks in before the ultralight mode Yukawa suppression develops. The ultralight graviton mass still feeds the running of G_{eff} , yielding large distance decay as⁵ $\exp[-(2 + \ell^2 m^2/3)r/\ell]$. This postpones the deviations from $4D$ to $\mathcal{R} > \ell/(\ell^2 m^2) \sim \ell^3/L^2$.

Our findings are consistent with the interpretation of locally localized gravity in terms of a defect CFT proposed in [11, 20]. In the picture where the defect is “fat” the CFT is cut off in the UV at its inverse thickness, $1/L$. When the cutoff is fixed to some finite value, the local geometry becomes dynamical, described by $4D$ gravity whose Planck mass is set by the cutoff. The defect excitations are described by an effective conformal field theory emerging from the dual CFT mixing with the defect, but whose conformal symmetry breaks to $SO(3, 2)$ at a low scale $1/\ell$, generated by the strong coupling dynamics of the system. These degrees of freedom are light and interact with the $4D$ graviton giving it a small, radiatively generated mass $m^2 \sim g_* \frac{1}{M_4^2} \frac{1}{\ell^4} \sim \frac{L^2}{\ell^4}$ [19]. We find that they also must renormalize the $4D$ Newton’s constant by IR contributions, which correspond to the terms in the L/ℓ expansion of our formula (1.1): $M_4^2 = M_5^3 L \left(1 + \frac{5}{12}(\frac{L}{\ell})^2 + \dots\right)$. They also dress up the $4D$ Newton’s constant with external momentum-dependent terms, which make the graviton look composite at distances below ℓ . Far from the source the effective Newton’s constant goes to zero as distance increases at a rate set by the anomalous dimension of the operator which should be dual to the graviton in $AdS_4 \subset AdS_5$. This suggests a link with the holographic rescaling in the boundary CFT [27].

The paper is organized as follows. In the next section we develop the formalism needed to construct the shock waves on $AdS_4 \subset AdS_5$. In section 3 we derive the shock wave profile in a closed form. We explore the limits of the solution in section 4, and derive the Planck mass formula (1.1) and explore the four relevant dynamical regimes, outlining the limit $\ell \rightarrow \infty$ which takes the theory to RS2. We discuss the connection with AdS/CFT in section 5 and summarize in section 6. In the appendices

⁵This formula is a dimensional hybrid: the factor 2 comes from AdS_4 , and $1/3$ from AdS_5 dynamics. The latter is the culprit of mimicking the “running” of G_N we mention above. See below.

we give some details of the derivation of the wave profile field equation, the limiting cases of the solution and the spectrum of localized gravitons.

2. Setup

Generalizations of the Aichelburg-Sexl waves, describing a relativistic particle in a $4D$ flat space [21, 22], to curved spaces and to more dimensions, as well as the properties of the solutions, have been considered in [28, 29, 30, 31, 32, 33, 34, 35, 36, 37, 38]. As in those cases, we find that the gravitational field equations reduce to a single *linear* partial differential equation for the shock wave. We follow the cutting-and-pasting trick of Dray and 't Hooft [28], adopted to de Sitter and AdS backgrounds by Sfetsos [34], and recently employed by one of us in the construction of exact shock waves [37] in DGP braneworlds [39]. Many of the results of [37] carry over with minor changes. That is, we start with a background determining a tensional 3-brane residing in AdS_5 bulk such that the induced geometry on the brane is AdS_4 . We perturb it with a photon, which moves along a null geodesic with a momentum $p = 2\pi\nu$. Its momentum generates a gravitational field, since it contributes to the total stress-energy tensor. Because of the infinite boost, the gravitational field of the particle will be completely confined to the instantaneous plane orthogonal to the direction of motion, and the Einstein's equations will break up into the background equations and a single field equation for the wave profile. This equation is linear by the analyticity of the setup. This can be seen from imagining a solution for a massive source and expanding the exact metric in a Taylor series in the mass m , and boosting it to relativistic speeds, by enforcing $\cosh \gamma \rightarrow \infty$, $m \rightarrow 0$ and $m \cosh \gamma = p = \text{const}$. Only the linear terms in m in the expansion survive in this limit because there is only one factor of the boost parameter $\cosh \gamma$ in the metric, which will be overcompensated by higher powers of m . The linearized solution becomes exact, implying that the only nontrivial field equation must be linear. If we choose coordinates such that v runs along the photon null geodesic and u orthogonally to it, such that the world-line of the particle is $u = 0$, then by causality the field experiences a jump at $u = 0$. The gravitational field of the particle jolts the observer exactly at the moment when the particle flies by her [28].

Our starting point is, as in [37], the $5D$ metric describing the background, in this case $AdS_4 \subset AdS_5$ [4, 7], which can be written as a warped product of AdS_4 :

$$ds^2_{AdS_5} = \frac{L^2}{\ell^2 \sin^2(\frac{|z|+z_0}{\ell})} \left[ds^2_{AdS_4} + dz^2 \right]. \quad (2.1)$$

In this equation the parameter z_0 , determining the conformal distance of the brane from the center of the bulk (i.e. the warp factor “bounce”) is given by $\sin(z_0/\ell) = L/\ell$.

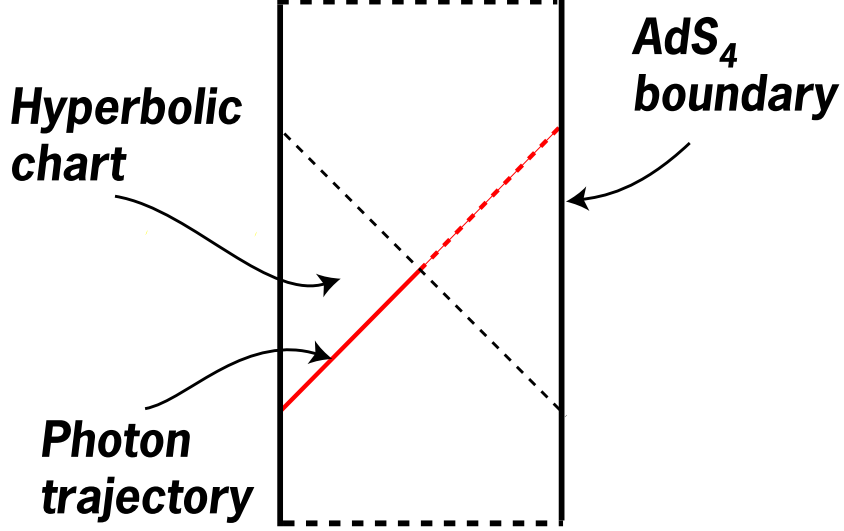


Figure 1: AdS_4 strip. Patch of AdS_4 covered by Eq. (2.2), designated “Hyperbolic chart”, and the photon trajectory. The bold red line depicts the part of the photon trajectory covered by the chart on which the metric (2.2) is defined, and the dashed red line segment is its future extension.

This is just the Israel junction condition in disguise. Following [34], we choose a patch of AdS_4 covered with the static coordinates foliated by hyperbolic hyper-planes,

$$ds^2_{AdS_4} = -\left(\frac{r^2}{\ell^2} - 1\right) dt^2 + \frac{dr^2}{\frac{r^2}{\ell^2} - 1} + r^2 \left(d\chi^2 + \sinh^2 \chi d\phi^2\right). \quad (2.2)$$

These coordinates cover the region of AdS_4 enclosed by the AdS_4 boundary and the two null cones balancing on each other’s tips, as depicted in Fig. (1). Note that while the AdS_4 boundary is at $r \rightarrow \infty$, the center is at $r = \ell, |t| \neq \infty$. The surfaces $r = \ell, t \rightarrow \pm\infty$ are Cauchy horizons. This is the correct AdS_4 domain, bounded by the null geodesics along which we will introduce the discontinuity à la Dray-’t Hooft [34] (see also [33] for a discussion of the shape of shocks in AdS). The null coordinates are given by the map

$$u = \ell e^{t/\ell} \left(\frac{r - \ell}{r + \ell}\right)^{1/2}, \quad v = \ell e^{-t/\ell} \left(\frac{r - \ell}{r + \ell}\right)^{1/2}. \quad (2.3)$$

In terms of these coordinates we can rewrite the brane AdS metric (2.2) as

$$ds^2 = \Omega^2(|z|) \left[\frac{4 du dv}{(1 - uv/\ell^2)^2} + \ell^2 \left(\frac{1 + uv/\ell^2}{1 - uv/\ell^2}\right)^2 (d\chi^2 + \sinh^2 \chi d\phi^2) + dz^2 \right]. \quad (2.4)$$

We introduce the warp factor $\Omega(|z|) = \left[L / [\ell \sin(\frac{|z| + z_0}{\ell})] \right]$ as a shorthand notation.

Enter the photon. We choose the v -axis of (2.4) as its trajectory, i.e. the null geodesic $u = 0$. That is depicted as the red null line in Fig. (1). Then following Dray and 't Hooft we change the metric by including a jump in the v coordinate at $u = 0$ [28]. This encodes the shock wave profile. To do this, we can replace v, dv in (2.4) by

$$v \rightarrow v + \Theta(u)f, \quad dv \rightarrow dv + \Theta(u)df, \quad (2.5)$$

where f is the shock wave profile, which is required to solve the field equations with the photon contribution to the stress-energy tensor included on the right hand side (RHS). As before the wave profile f depends only on the spatial coordinates transverse to the trajectory of the source, which in our case are the coordinates on \mathcal{H}_2 and the bulk coordinate z . Here $\Theta(u)$ is the Heaviside step function. It is convenient to slightly change the coordinates to $\hat{v} = v + \Theta(u)f$, in which case $dv \rightarrow d\hat{v} - \delta(u)fdu$. Dropping carets, we substitute these in (2.4), yielding the metric Ansatz which includes the shock wave profile:

$$ds^2 = \Omega^2(|z|) \left[\frac{4 du dv}{(1 - uv/\ell^2)^2} - \frac{4\delta(u)fdu^2}{(1 - uv/\ell^2)^2} + \ell^2 \left(\frac{1 + uv/\ell^2}{1 - uv/\ell^2} \right)^2 (d\chi^2 + \sinh^2 \chi d\phi^2) + dz^2 \right]. \quad (2.6)$$

Next we substitute Eq. (2.6) into the field equations

$$G_{5B}^A = \frac{6}{L^2} \delta^A_B - 6 \left(\frac{1}{L^2} - \frac{1}{\ell^2} \right)^{1/2} \delta^\mu_\nu \delta_\mu^A \delta_B^\nu \delta(z) + 2 \frac{p}{M_5^3} \frac{g_{4uv}}{\sqrt{g_5}} \delta^\mu_\nu \delta_\nu^u \delta_\mu^A \delta_B^\nu \delta(\chi) \delta(\phi) \delta(u) \delta(z). \quad (2.7)$$

We include the brane-localized terms as $\delta(z)$ -function sources on the RHS because the metric (2.6) is in the Gaussian-normal form, and $\sqrt{g_4/g_5} = 1/\Omega = 1$ at the location of the brane $z = 0$. We also include the photon stress-energy contribution, $\propto p$, in the source on the RHS, and pick the coordinates on \mathcal{H}_2 such that the photon trajectory is along $\chi = \phi = 0$. In the equation, G_{5B}^A is the bulk Einstein tensor evaluated on (2.6), indices $\{A, B\}$ and $\{\mu, \nu\}$ are bulk and brane worldvolume indices, respectively, and $g_{4\mu\nu}$ is the induced metric on the brane, in this case simply the obvious restriction of g_{AB} to $g_{\mu\nu}$. We have traded the brane tension λ from the equation using the relation between it and the bulk and brane curvature radii [4], $\lambda = 6M_5^3 \left(\frac{1}{L^2} - \frac{1}{\ell^2} \right)^{1/2}$. One can easily check that the photon stress-energy is automatically conserved, $\nabla_\mu T^\mu_{\nu \text{ photon}} \propto u\delta(u) = 0$, as it must be by Bianchi identities. Relegating the details to the Appendix A, here we merely quote the result of this computation: the *linear* field equation for the wave profile is

$$\partial_z^2 f + 3 \frac{\partial_{|z|} \Omega}{\Omega} \partial_{|z|} f + \frac{1}{\ell^2} (\Delta_2 f - 2f) = \frac{2p}{M_5^3 \ell^2} \delta(\cosh \chi - 1) \delta(\phi) \delta(z) \quad (2.8)$$

where the operator Δ_2 is the Laplacian on the “unit” hyperbolic surface \mathcal{H}_2 . This equation arises from the $u-v$ component of (2.7), whereas all others are simple identities by virtue of the relation $L/\ell = \sin(z_0/\ell)$. Now we can turn to solving (2.8).

3. Shocks

The wave profile can only depend on the transverse spacelike coordinates z, χ, ϕ . Having picked the transverse coordinates such that the photon trajectory is along $\chi = \phi = 0$ in the \mathcal{H}_2 hyperplane, we need only look at the bottom portion of the trajectory, starting at the AdS_4 boundary and ending at the AdS_4 center. These coordinates provide a natural description of the shock wave profiles in AdS_4 because the planes $t, r = \text{const}$ are hyperbolic, exactly the shape of the shock wave surfaces [33, 34]. This is the part in the past of the chart covered by the coordinates featuring in the metric (2.4), as depicted by the bold red line in Figure (1). Indeed, since the photon trajectory is $u = 0$, from (2.3) we see that it zips along $r = \infty, t \rightarrow -\infty$ from the AdS_4 boundary to its center. We can easily extend the trajectory beyond the AdS_4 center, mapping it to the future portion by a global AdS_4 rotation and a time reversal. Then, from the axial symmetry around the photon trajectory, we expect that the wave profile should be independent of ϕ , thanks to our choice of coordinate system in the transverse \mathcal{H}_2 . This is all borne out by the solution, as we will now show.

In the expanded form, using $\Delta_2 = \partial_\chi^2 + \coth \chi \partial_\chi + \frac{\partial_\phi^2}{\sinh^2 \chi}$ the wave profile equation (2.8) reads

$$\begin{aligned} \partial_y^2 f - 3 \cot(|y| + y_0) \partial_{|y|} f + \left(\partial_\chi^2 f + \coth \chi \partial_\chi f + \frac{\partial_\phi^2 f}{\sinh^2 \chi} - 2f \right) = \\ = \frac{2p}{M_5^3 \ell} \delta(\cosh \chi - 1) \delta(\phi) \delta(y), \end{aligned} \quad (3.1)$$

where we introduce $y = z/\ell$, $y_0 = z_0/\ell = \arcsin(L/\ell)$ to simplify the subsequent manipulations.

This equation is separable. We therefore seek for solutions of the form

$$f(y, \chi, \phi) = \sum_m \int dq \psi_{q,m}(y) H_{q,m}(\chi, \phi). \quad (3.2)$$

The functions $H_{q,m}(\chi, \phi)$ are the eigenfunctions of the Laplacian on \mathcal{H}_2 ,

$$\Delta_2 H_{q,m}(\chi, \phi) = - \left(q^2 + \frac{1}{4} \right) H_{q,m}(\chi, \phi). \quad (3.3)$$

They are defined by [40, 41]

$$H_{q,m}(\chi, \phi) = e^{im\phi} Z_{q,m}(\chi), \quad Z_{q,m}(\chi) \equiv \frac{\Gamma(iq + m + 1/2)}{\Gamma(iq)} P_{iq-1/2}^{-m}(\cosh \chi). \quad (3.4)$$

They are an orthonormal basis on \mathcal{H}_2 by $\int_0^\infty d\chi \sinh \chi Z_{q,m}(\chi) Z_{q',m}^*(\chi) = \delta(q - q')$, $\int d\phi e^{im\phi} e^{-im'\phi} = 2\pi \delta_{m,m'}$. Note that $H_{q,m}(\chi, \phi)$ are the generalization of spherical harmonics $Y_{q,m}(\theta, \phi)$ to the hyperplane \mathcal{H}_2 . Their completeness relation [41] with our choice of coordinate system on \mathcal{H}_2 yields

$$\sum_{m=-\infty}^{\infty} \int_0^\infty d\chi H_{q,m}(\chi, \phi) H_{q,m}^*(0, 0) = \delta(\cosh \chi - 1) 2\pi \delta(\phi). \quad (3.5)$$

Inserting this for $\delta(\cosh \chi - 1) \delta(\phi)$ in (3.1) and using the orthonormality of the eigenmodes, we get the equation for the radial bulk modes $\psi_{q,m}$. The Fourier coefficients of the $\delta(\cosh \chi - 1) \delta(\phi)$ in this basis obey $Z_{q,0}^*(0) = \Gamma(-iq + 1/2)/\Gamma(-iq)$, $Z_{q,m \neq 0}^*(0) = 0$, and so only the axially symmetric modes, $m = 0$, will have a nonzero source. Since we are only interested in the field of the photon, carried by its momentum p , and not in the homogeneous modes, we set $\psi_{q,m \neq 0} = 0$ for all q . Hence the equation for the axially symmetric modes, $\psi_q(y) \equiv \psi_{q,0}(y)$, is

$$\partial_y^2 \psi_q(y) - 3 \cot(|y| + y_0) \partial_{|y|} \psi_q(y) - \left(q^2 + \frac{9}{4}\right) \psi_q(y) = \frac{p}{\pi M_5^3 \ell} \frac{\Gamma(-iq + 1/2)}{\Gamma(-iq)} \delta(y) \quad (3.6)$$

One linearly independent set of eigenmodes of the operator on the LHS is given by the Legendre functions

$$\sin^2(|y| + y_0) P_{iq-1/2}^{-2}(\cos(|y| + y_0)), \quad \sin^2(|y| + y_0) Q_{iq-1/2}^{-2}(\cos(|y| + y_0)). \quad (3.7)$$

Notice that in spite of the appearances, these functions are real. With our coordinate choices, the AdS_5 boundary lies at $|y_b| + y_0 = \pi$. Thus locally localized gravity corresponds to the linear combination of these two modes which remains regular as the argument of P_ν^{-2} and Q_ν^{-2} approaches -1 . To find that combination, we expand the modes in the limit $\cos(|y| + y_0) = x \rightarrow -1^+$, where

$$P_\nu^{-2}(x) = \frac{2}{\Gamma(3 + \nu) \Gamma(2 - \nu)} \frac{1}{1 + x}, \quad Q_\nu^{-2}(x) = -\frac{\cos(\pi\nu) \Gamma(\nu - 1)}{\Gamma(\nu + 3)} \frac{1}{1 + x}. \quad (3.8)$$

The linear combination which is regular at the AdS_5 boundary, and so describes the localized graviton modes, is proportional to [42]

$$\cos(\pi\nu) P_\nu^{-2}(\cos(|y| + y_0)) + 2 \frac{Q_\nu^{-2}(\cos(|y| + y_0))}{\Gamma(\nu - 1) \Gamma(2 - \nu)} = P_\nu^{-2}(-\cos(|y| + y_0)). \quad (3.9)$$

Therefore, the localized graviton modes are

$$\psi_q(y) \equiv N_q \sin^2(|y| + y_0) P_{iq-1/2}^{-2}(-\cos(|y| + y_0)) . \quad (3.10)$$

The normalization constant N_q is determined by a pillbox integration of the equation (3.6), imposing the Z_2 orbifold boundary conditions on the brane at $y = 0$. This gives

$$\psi'_q(0) = \frac{p}{2\pi M_5^3 \ell} \frac{\Gamma(-iq + 1/2)}{\Gamma(-iq)} , \quad (3.11)$$

and, using the identity $(\sin^2 \xi P_\nu^{-2}(-\cos \xi))' = -\sin^2 \xi P_\nu^{-1}(-\cos \xi)$ we finally obtain

$$N_q = -\frac{p \ell}{2\pi M_5^3 L^2} \frac{\Gamma(-iq + 1/2)}{\Gamma(-iq)} \left[P_{iq-1/2}^{-1}(-\cos(y_0)) \right]^{-1} . \quad (3.12)$$

Therefore our complete solution describing the shock wave profile is given by the integral formula

$$f(y, \chi) = -\frac{p \ell}{2\pi M_5^3 L^2} \int_0^\infty dq q \tanh(\pi q) \times \\ \times \sin^2(|y| + y_0) \frac{P_{iq-1/2}^{-2}(-\cos(|y| + y_0))}{P_{iq-1/2}^{-1}(-\cos(y_0))} P_{iq-1/2}(\cosh \chi) , \quad (3.13)$$

where we have used $|\Gamma(iq + 1/2)/\Gamma(iq)|^2 = q \tanh \pi q$. On the brane, at $y = 0$, the integral formula (3.13) reduces to

$$f(0, \chi) = -\frac{p}{2\pi M_5^3 \ell} \int_0^\infty dq q \tanh(\pi q) \frac{P_{iq-1/2}^{-2}(-\cos(y_0))}{P_{iq-1/2}^{-1}(-\cos(y_0))} P_{iq-1/2}(\cosh \chi) . \quad (3.14)$$

These two equations represent our main technical results. We now turn to extracting physics from them.

4. Limits

Using the integral formula (3.14) we can now probe the shock wave profile along the brane as a function of the transverse distance from the photon which sources the field. We compare the result in different regimes with the form of the shock wave in conventional GR in $5D$ and $4D$ to elucidate the nature of localized gravity. Note that in general this approach could be suspect because of the issues of gauge choice, related to the choice of the background metric. However because the relativistic source excites only the transverse traceless gravitons, and the gravitational dynamics linearizes in this

limit, no gauge ambiguities arise in any coordinate cover of $AdS_4 \subset AdS_5$. The transverse traceless nature of the shock ensures that we are working in the unitary gauge and that information extracted from the shock wave describes the physical gravitons of the theory, independently of the background coordinates. Simply put, the shock wave amplitude which we compute is the static limit of the physical Green's function of the tensor graviton resonance in the hyperplane transverse to the motion of the relativistic source [24, 25]. The discussion below will elaborate this further.

We still need to define a measure of the transverse distance \mathcal{R} from the source in the background metric (2.6). We note that the metric transverse to the photon on the brane is $ds_2^2|_{z=u=0} = \ell^2 (d\chi^2 + \sinh^2 \chi d\phi^2)$. Thanks to the axial symmetry of (2.1) we need only consider variation of f with the “radial” transverse distance on \mathcal{H}_2 . Thus we should scan the wave variation with χ . The proper radial distance from the source is therefore measured by $\mathcal{R} = \ell\chi$. At very large distances $\chi \gg 1$ where we can't neglect the AdS_4 curvature, the warping of AdS_4 changes the measure of angular distances to the exponent $\exp(\chi) = \exp(\mathcal{R}/\ell)$, but we needn't pay a particular attention to it here thanks to the axial symmetry of the shock waves.

4.1 Surfing the Wave

Now, to test locally localized gravity we need to define the benchmarks to compare our shock wave solution (3.14) to. At short distances, we should compare it to the 5D version of the Aichelburg-Sexl wave, derived in [29, 30]

$$f_{5D}(\mathcal{R}) = -\frac{p}{2\pi M_5^3} \frac{1}{\mathcal{R}}. \quad (4.1)$$

At large distances $\mathcal{R} > L$, the most convenient form of the shock wave in AdS_4 for our purposes is the one derived by Sfetsos [34],

$$f_{4D \text{ AdS}}(\chi) = -\frac{p}{\pi M_4^2} Q_1(\cosh \chi). \quad (4.2)$$

This solution describes the 4D *GR* shock wave at all length scales in AdS_4 , and correctly reproduces the 4D Aichelburg-Sexl wave in flat space at short distances $\mathcal{R} \ll \ell$, where AdS_4 curvature is negligible⁶:

$$f_{4D \text{ A-S}} = \frac{p}{\pi M_4^2} \log \frac{\mathcal{R}}{2\ell} + \frac{p}{\pi M_4^2} + \dots. \quad (4.3)$$

Both solutions (4.2), (4.3) will provide useful standards for our ends. Before we continue with the comparisons it is useful to review the salient features of the spectrum of locally localized gravity.

⁶While the constant in (4.3) is gauge-dependent in flat space, the gauge is uniquely fixed by the choice of the normalization of \mathcal{R} under the logarithm [28]. We will use it later, when discussing the limit to RS2.

4.1.1 Spectral Decomposition of the Shock Wave

Let us briefly review some useful mathematical tools before exploring the physics of the shock wave. First, it is convenient to re-express the integral on the RHS of (3.14) as a sum. The series representation of (3.14) is (for details see Appendix B):

$$f(0, \chi) = \frac{p}{2\pi M_5^3 \ell} \sum_{\nu > -1/2} (2\nu + 1) \frac{P_\nu^{-2}(-\cos(y_0))}{\partial_\nu P_\nu^{-1}(-\cos(y_0))} Q_\nu(\cosh \chi) . \quad (4.4)$$

The sum runs over all the values of $\nu \equiv iq - 1/2$ that solve

$$P_\nu^{-1}(-\cos(y_0)) = 0 , \quad (4.5)$$

with the condition $\nu > -1/2$. This is an exact statement, no approximations have been made in writing (4.4), (4.5).

The equation (4.4) is the graviton mode expansion of the shock wave profile. We note that the expression (4.5) is the secular equation of the problem, determining the spectrum of gravitons in locally localized gravity. This can be verified easily from the homogeneous equation of (3.6), which is

$$\partial_y^2 \psi(y) - 3 \cot(|y| + y_0) \partial_{|y|} \psi(y) = m^2 \ell^2 \psi(y) , \quad (4.6)$$

after substituting $m^2 = \frac{\nu(\nu+1)-2}{\ell^2}$. Upon setting $p = 0$, the boundary condition (3.11) reduces to the Neumann boundary condition

$$\psi'_q(0) = 0 . \quad (4.7)$$

Plugging in the localized graviton wave functions (3.10), we find that those which satisfy (4.7) are counted by the index q , defined such that $\nu = iq - 1/2$ solves (4.5) for a fixed y_0 . They yield the mass spectrum through the relation of ν and the graviton mass m . The graviton couplings are given by the coefficients of $Q_\nu(\cosh \chi)$ in the series (4.4):

$$g_n^2 = \frac{2\nu + 1}{2M_5^3 \ell} \frac{P_\nu^{-2}(-\cos(y_0))}{[-\partial_\nu P_\nu^{-1}(-\cos(y_0))]} \Big|_{\nu=\nu_n} . \quad (4.8)$$

The (-) sign cancels another (-) sign concealed in $\partial_\nu P_\nu^{-1}$. This is the exact formula for the couplings of each individual graviton mode to the matter on the brane in terms of the 5D Planck mass and the curvature radii L and ℓ .

We can find the explicit values of the masses and couplings in the limit $L \ll \ell$ (see Appendix C for the derivation). For ultralight and intermediate modes, $\nu_n \simeq$

$n + \frac{L^2}{4\ell^2} n(n+1)$ (C.5), whereas for heavy modes $\nu_n \simeq n \left(1 + \frac{L^2}{\pi\ell^2}\right)$ (C.8). The low end masses are

$$m^2 = \frac{1}{\ell^2} \left[(n-1)(n+2) + \frac{1}{2} n(n+1/2)(n+1) \frac{L^2}{\ell^2} \right] + \dots, \quad n = 1, 2, 3, \dots \quad (4.9)$$

The ultralight mode of mass $m = \sqrt{\frac{3}{2}} \frac{L}{\ell^2} + \dots$ appears at $n = 1$, as in [9]. The masses of intermediate modes are $m \sim \sqrt{(n-1)(n+2)}/\ell$. The masses of heavy modes are (see (C.8))

$$m^2 = \frac{1}{\ell^2} \left[n^2 + n + \frac{2L^2}{\pi\ell^2} n^2 \right] + \dots, \quad n \gtrsim \frac{\ell}{L}. \quad (4.10)$$

The heavy modes reside above the UV cutoff $1/L$, $m \gtrsim 1/L$, of the dual CFT , where the CFT breaks down, but are still well defined on the bulk side as long as $L \ll 1/M_5$. They are effectively decoupled at all distances $\mathcal{R} > L$. The couplings of light and intermediate modes are (see Appendix C)

$$g_n^2 = \frac{L}{4M_5^3\ell^2} \frac{(2n+1)n(n+1)}{n+2} \frac{1}{n-1+n(n+1)(L^2/4\ell^2)} + \dots, \quad n \geq 1. \quad (4.11)$$

The ultralight mode is *much* more strongly coupled than the rest, because

$$g_1^2 = \frac{1}{M_5^3 L} + \dots, \quad (4.12)$$

just as in RS2, while the couplings of heavier modes are suppressed relative to it by two extra powers of L/ℓ :

$$g_m^2 \simeq \frac{mL}{2M_5^3\ell} + \dots \quad (4.13)$$

This formula eventually saturates to $g_m^2 \simeq \frac{1}{M_5^3\ell}$ at the high end of the spectrum.

We will also need the short and long distance behavior of Q_{ν_n} 's in order to interpret the physical meaning of the series (4.4). Short distance limit corresponds to $\chi \ll 1$, in which case we can use the expansion [42]

$$Q_{\nu_n}(\cosh \chi) \simeq -\log \chi/2 - \psi(\nu_n + 1) - \gamma_E + \mathcal{O}(\chi^2) + \mathcal{O}(\chi^2 \ln \chi) + \dots, \quad (4.14)$$

where γ_E is Euler-Mascheroni constant, and $\psi(\nu_n + 1)$ the digamma function [43]. It is clear that as χ increases, the logarithm decreases, and at some point it stops to dominate. Because the ψ function is approximated by $\psi(\nu_n + 1) \simeq \log \nu_n$ for large values of ν_n , the expansion (4.14) is valid when the first term dominates over the second, $\nu_n < 2/\chi$. Since $m \sim \nu_n/\ell$ for intermediate and massive modes (4.9), (4.10), the approximation of their mode functions (4.14) is valid to distances $\mathcal{R} < 2/m$. On

the other hand, for the ultralight mode its mass $m \sim L/\ell^2$ does not affect the mode function until much farther out, but the approximation (4.14) still breaks down at $\mathcal{R} \lesssim \ell$ even for it.

To understand their behavior at very large transverse distances from the source, we need a different asymptotic formula for functions $Q_{\nu_n}(\cosh \chi)$. At $\chi \gg 1$ the leading order behavior is [42]

$$Q_{\nu_n}(\cosh \chi) = \sqrt{\pi} \frac{\Gamma(1 + \nu_n)}{\Gamma(3/2 + \nu_n)} e^{-(1+\nu_n)\chi} + \dots \quad (4.15)$$

The scaling $\sim \exp[-(1 + \nu_n)\chi]$ is dictated by the mass and the *AdS* geometry, as is seen from the mode equation on \mathcal{H}_2 , that follows from (3.1) by setting the RHS to zero, separating out the bulk dependence by using (4.6) and substituting $2 + m^2\ell^2 = \nu_n(\nu_n + 1)$. The resulting mode equation on \mathcal{H}_2 is

$$\left(\partial_\chi^2 + \frac{\cosh \chi}{\sinh \chi} \partial_\chi - \nu_n(\nu_n + 1) \right) Q = 0. \quad (4.16)$$

It's easy to check that the asymptotic limit (4.15) is the large χ limit of the solution which is regular at infinity. Rewriting (4.15) in terms of the mode mass by using $\nu_n = (\sqrt{9 + 4m^2\ell^2} - 1)/2$ for localized solutions we get

$$Q_{\nu_n}(\cosh \chi) = \sqrt{\pi} \frac{\Gamma\left(\frac{\sqrt{9+4m^2\ell^2}+1}{2}\right)}{\Gamma\left(\frac{\sqrt{9+4m^2\ell^2}+2}{2}\right)} \exp\left(-\frac{\sqrt{9+4m^2\ell^2}+1}{2}\chi\right) + \dots \quad (4.17)$$

The intermediate and heavy mode masses are $m^2\ell^2 > 1$, and so they will drop off as $\propto \exp[-(m\ell + \frac{1}{2})\chi]$, feeling conventional Yukawa suppressions. This is obvious for the modes with masses $m\ell \gtrsim \mathcal{O}(10)$, but even for the few lighter ones it's clear that Yukawa term cannot be ignored.

On the other hand, for the ultralight mode $m^2\ell^2 \sim (L/\ell)^2 \ll 1$, and so at large distances, the ultralight mode function scales to the leading order as $\propto \exp(-2\chi)$. What that means is, the ultralight mode function at large distances is predominantly controlled by the *AdS*₄ geometry, in qualitatively the same way light bulk modes in *AdS/CFT*. Indeed, for the ultralight graviton we can rewrite (4.17) approximately as

$$Q_{\nu_n}(\cosh \chi) = \frac{4}{3} e^{-(2+\frac{m^2\ell^2}{3})\chi} + \dots \quad (4.18)$$

Using $\mathcal{R} = \ell\chi$, this means that the mass remains negligible all the way out to distances $\mathcal{R} \gtrsim \ell/(m^2\ell^2) \simeq \ell^3/L^2$, when it starts slowly “renormalizing” the coefficient $4/3$ of $e^{-2\chi}$. So unlike for the heavier modes, the regimes where the ultralight mode is well

described by (4.14) and by (4.15) *do not* overlap. Instead, the function Q_{ν_1} is extremely well approximated by Q_1 all the way out to ℓ^3/L^2 . Because $\nu_1 = 1 + \frac{L^2}{2\ell^2} + \dots$, writing

$$Q_{\nu_1}(\cosh \chi) = Q_1(\cosh \chi) + \frac{L^2}{2\ell^2} \partial_\nu Q_\nu(\cosh \chi) \Big|_{\nu=1} + \dots, \quad (4.19)$$

we find from (4.15) that since $\partial_\nu Q_\nu(\cosh \chi) \simeq \chi Q_\nu(\cosh \chi)$ the corrections to Q_1 indeed do remain small all the way out to $\frac{L^2}{\ell^2} \chi \gtrsim 1$, or therefore $\mathcal{R} \gtrsim \ell^3/L^2$.

To summarize: we see that for $n > 1$, the key features of Q_{ν_n} 's are captured by the representation

$$Q_{\nu_n} \simeq \begin{cases} -\log \frac{\mathcal{R}}{2\ell} - \psi\left(m\ell + \frac{1}{2}\right) - \gamma_E, & \text{for } \mathcal{R} < 2/m \quad ; \\ \sqrt{\pi} \frac{\Gamma(m\ell + \frac{1}{2})}{\Gamma(m\ell + 1)} e^{-(m\ell + \frac{1}{2})\frac{\mathcal{R}}{\ell}}, & \mathcal{R} > 2/m \quad . \end{cases} \quad (4.20)$$

The two limits practically overlap: at distances $\mathcal{R} \sim 2/m$, Q_{ν_n} sharply changes from a logarithm of the distance to a Yukawa-decaying exponential. On the other hand, the ultralight mode asymptotics is accurately captured by

$$Q_{\nu_1} \simeq \begin{cases} Q_1\left(\cosh\left(\frac{\mathcal{R}}{\ell}\right)\right), & \text{for } \mathcal{R} < \ell^3/L^2 \quad ; \\ \frac{4}{3} e^{-(2 + \frac{m^2\ell^2}{3})\frac{\mathcal{R}}{\ell}}, & \mathcal{R} > \ell^3/L^2 \quad , \end{cases} \quad (4.21)$$

never displaying Yukawa suppression.

With this at hand, we have the tools needed to complete the analysis of (4.4). First off, using (4.8) we can rewrite (4.4) as

$$f(0, \chi) = -\frac{p}{\pi} \sum_{n=1}^{\infty} g_n^2 Q_{\nu_n}(\cosh \chi) \quad . \quad (4.22)$$

We now need to extract $\propto Q_1$ contribution from (4.22) to compare it to the $4D$ forms of the shock wave (4.2), (4.3). The complication is that at distances $\mathcal{R} < \ell$ many massive modes contribute to it, as is clear for example from Eq. (4.14), which shows that each $Q_{\nu_n}(\cosh \chi)$ contains small tails $\propto Q_1(\cosh \chi)$. Indeed, the functions $Q_{\nu_n}(\cosh \chi)$ are *not* orthogonal [42]. However: from the qualitative expressions for Q_{ν_n} 's in Eqs. (4.20), (4.21) we know that the regions where they overlap with Q_1 are narrow, their width inversely proportional to the mass of the mode. Moreover, higher mode ($n > 1$) contributions are also coupling suppressed, by Eqs. (4.12), (4.13). Using this we can systematically extract physical information from the shock wave.

4.1.2 Short Distance Behavior

At distances $\mathcal{R} \ll L$ the shock wave reduces to the $5D$ version of Aichelburg-Sexl solution in flat space [29, 30]. We have to take the limit $\chi \ll 1$ of (3.14) cautiously, to

avoid spurious singularities that appear to plague the expression if χ were set to zero directly in the integrand. To do it, we integrate (3.14) first and then take the limit $\chi \rightarrow 0$. In this regime, the integral is dominated by its large q behavior, and so the leading short distance contributions come from the leading order q -dependence of the integrand. This is, of course, identical to the short distance limit considered in [37], because q/ℓ measures the momentum transfer between the source and a probe. At short distances it is large, and so the shock wave is dominated by the heavy gravitons whose sheer number overwhelms all other modes. Using [43] (see Eqs. (8.721.1) and (8.723.1)) we can expand

$$\begin{aligned} \frac{P_{iq-1/2}^{-2}(-\cos(y_0))}{P_{iq-1/2}^{-1}(-\cos(y_0))} &= 1/q + \dots, \\ P_{iq-1/2}(\cosh \chi) &= \frac{1}{\sqrt{\pi}} \left[\frac{\Gamma(iq)}{\Gamma(1/2 + iq)} \frac{e^{(iq+1/2)\chi}}{\sqrt{e^{2\chi} - 1}} + \text{h.c.} \right] + \dots, \end{aligned} \quad (4.23)$$

and, after using asymptotic expansions for Γ -functions and rescaling $q = \zeta/\chi$, we finally find the leading order contribution to be

$$f(0, \chi \ll 1) = -\frac{p}{2\pi M_5^3 \ell \chi} \sqrt{\frac{2}{\pi}} \int_0^\infty d\zeta \frac{\sin(\zeta)}{\sqrt{\zeta}}. \quad (4.24)$$

This integral is easy, it is just $\sqrt{\pi/2}$. Using $\mathcal{R} = \ell\chi$ we finally get

$$f_{\text{short distance}} = -\frac{p}{2\pi M_5^3} \frac{1}{\mathcal{R}}. \quad (4.25)$$

Thus as anticipated we exactly recover the 5D Minkowski space shock wave profile (4.1) of [29, 30]. This is a nice consistency check of the method and the calculation.

4.1.3 Composite Graviton Regime

When $\mathcal{R} > L$, the best form of our solution to work with is the mode expansion (4.22). To explore this region we start with $\mathcal{R} \ll \ell$ and move out. In this regime the relevant 4D benchmark to compare (4.22) to is the limiting form of (4.2) given, to the leading order, by the 4D Aichelburg-Sexl shock wave (4.3). For a fixed $\mathcal{R} \ll \ell$, we see from Eq. (4.20) that all the gravitons with masses $m > 2/\mathcal{R}$ are effectively decoupled because of the Yukawa suppression: their contribution to (4.22) is exponentially suppressed, $\propto \exp(-m\mathcal{R})$, over and above the coupling suppressions of (4.13). Thus we can truncate the sum in (4.22) to $m < 2/\mathcal{R}$, or alternatively to $n \lesssim 2\ell/\mathcal{R}$ (which will clearly still involve many terms for a small \mathcal{R}). The leading contribution of all of these modes to

(4.22) will be $\propto \frac{p}{\pi} g_n^2 \log \frac{\mathcal{R}}{2\ell}$, and so we conclude that the leading term in (4.22) will be of the form

$$f_0 = \frac{p}{\pi} \left(g_1^2 + \sum_{n=2}^{m_{max} < 2/\mathcal{R}} g_n^2 \right) \log \frac{R}{2\ell} + \frac{p}{\pi} \left(g_1^2 [\psi(\nu_1 + 1) + \gamma_E] + \sum_{n=2}^{m_{max} < 2/\mathcal{R}} g_n^2 [\psi(\nu_n + 1) + \gamma_E] \right) + \dots \quad (4.26)$$

Here we also retain subleading corrections to compare with the limiting case of shock wave in RS2 later on. By Eqs. (4.12), (4.13) we can write $g_n^2 = \frac{L}{2\ell} m L g_1^2 + \dots$, so that

$$f_0 = \frac{p}{\pi} g_1^2 \left(1 + \frac{1}{2} \sum_{n=2}^{m_{max} < 2/\mathcal{R}} \frac{L}{\ell} m L + \dots \right) \log \frac{R}{2\ell} + \frac{p}{\pi} \left(g_1^2 [\psi(\nu_1 + 1) + \gamma_E] + \sum_{n=2}^{m_{max} < 2/\mathcal{R}} g_n^2 [\psi(\nu_n + 1) + \gamma_E] \right) + \dots \quad (4.27)$$

Comparing (4.27) with (4.3), one can identify the coefficient of the logarithm in (4.27) with the 4D effective gravitational coupling,

$$G_{eff} = g_1^2 \left(1 + \frac{1}{2} \sum_{n=2}^{m_{max} < 2/\mathcal{R}} \frac{L}{\ell} m L + \dots \right). \quad (4.28)$$

The logic behind this is that in 4D GR, the shock wave is the Fourier transform of the gravitational elastic forward scattering amplitude between the source and the probe [24, 25]. Thus if we took (4.27), Fourier-transformed it to the momentum picture, and factored out the leading order momentum dependence characterizing the 4D interaction, the remainder would measure the interaction strength at a given scale. In quantum field theory such identification yields a coupling which is *scale-dependent* when loops are included: because of renormalization effects, it depends on the energy scale, or its conjugate distance scale, at which it is measured. The scale dependence in (4.28) however arises as a purely classical effect: it is weakly dependent on the distance scale \mathcal{R} at which the probe is deflected by the shock wave, because the probe interacts with the fields of many KK gravitons in addition to the ultralight mode. As distance increases, more intermediate gravitons drop out from (4.27) due to Yukawa suppression from their mass, and G_{eff} changes with distance, weakly and in almost discrete jumps, thanks to the fact that the intermediate mode functions change from a logarithm to a Yukawa-suppressed form very sharply (4.20). After every distance step of $\sim 2\ell/n$, G_{eff}

would jump by $\frac{\Delta G_{eff}}{G_{eff}} \sim n \frac{L^2}{2\ell^2} \sim \frac{L^2}{\ell \mathcal{R}}$, staying practically constant for a long distance thereafter. The jumps are the largest at short scales, but $\frac{\Delta G_{eff}}{G_{eff}} \lesssim \frac{L}{\ell}$ as long as $\mathcal{R} > L$.

Note that if we view (4.28) as a series in the powers of L/ℓ , and substitute the formula for g_1^2 (4.8) also expanded in the powers of L/ℓ , using (4.12) to extract the leading term we would obtain the expansion

$$G_{eff} = \frac{1}{M_5^3 L} \left(1 + \dots\right) \left(1 + \frac{1}{2} \sum_{n=2}^{m_{max} < 2/\mathcal{R}} \frac{L}{\ell} m L + \dots\right), \quad (4.29)$$

where the factor $(1 + \dots)$ out front stands for the higher order L/ℓ corrections to g_1^2 . Note that the normalization of this expansion is by $M_4^2 = M_5^3 L$, precisely the formula for the Planck mass in RS2 [1]. We will discuss it in more detail in the following sub-section.

From (4.28) and the discussion leading to it we conclude that in this regime $4D$ gravity is *composite*: the shock wave behaves as a scattering amplitude generated by an exchange of a resonance composed from all intermediate gravitons with masses $m < 2/\mathcal{R}$, or *gravipartons*. The dominant contribution comes from the ultralight mode. The $4D$ effective gravitational coupling G_{eff} runs with scale, changing in well-separated sharp small jumps as long as $L \ll \ell$, because the intermediate gravitons are very weakly coupled and very light. Scattering of a probe particle against the shock probes the internal structure of the graviton resonance. As the distance increases towards ℓ , new distance dependent corrections induced by the AdS_4 curvature will become important, lifting the leading order shock wave to its AdS_4 form and obscuring the distance-dependent corrections generated by the intermediate gravipartons.

We note that except for the coupling suppression of intermediate and heavy modes, manifest in (4.13), this regime is analogous to the dynamics of gravity on a space with a large compact dimension at distances between the fundamental Planck length and the compactification radius [26]. As one increases the distance in the noncompact space, more and more KK modes drop out due to their masses, and the gravitational potential approaches the large distance limit set by the remaining light mode.

4.1.4 Ultralight Graviton Dominance

At distances $\ell \lesssim \mathcal{R} < \ell^3/L^2$ all the gravitons except the ultralight one have decoupled. Their contribution to (4.22) is exponentially small, due to Yukawa suppressions from their masses, as is clear from Eq. (4.20). The shock wave at these distances is completely composed of the ultralight mode, or in other words, the $4D$ graviton resonance is extremely narrow. The effects of the graviton mass are very small, as is clear from

either of the Eqs. (4.19) or (4.21). The shock wave profile is very closely approximated by

$$f_{\text{ultralight}}(0, \mathcal{R} \gtrsim \ell) = -\frac{p}{\pi} g_1^2 \left(1 - \mathcal{O}(1) \frac{L^2}{\ell^2} \chi\right) Q_1(\cosh \chi) + \dots \quad (4.30)$$

The leading χ dependence in (4.30) is identical to the AdS_4 shock wave of Sfetsos (4.2), provided that we identify g_1^2 with the 4D Planck mass M_4 , $g_1^2 = \frac{1}{M_4^2}$. In light of Eq. (4.8) this yields

$$M_4^2 = \frac{2M_5^3 \ell}{2\nu + 1} \frac{[-\partial_\nu P_\nu^{-1}(-\cos(y_0))]}{P_\nu^{-2}(-\cos(y_0))} \Big|_{\nu=\nu_0}, \quad (4.31)$$

where ν_0 is given by the ultralight mode mass according to $\nu_0 = [\sqrt{9 + 4\ell^2 m^2} - 1]/2$. We note that this definition is consistent with common practice in GR , where one identifies the Planck scale M_4^{-1} with the tree-level coupling of the lightest mode in the spectrum. In GR with a massless graviton this definition coincides with the one where the Planck scale is set by the gravitational scattering amplitude of two particles in the limit when their separation goes to infinity. Defined in this way, the Planck mass is a mere fixed dimensional parameter obtained as a limiting value of $G_{eff}^{-1/2}$ in the far infrared. This is still true in locally localized gravity: once we have defined M_4 as in Eq. (4.31), it is a dimensional parameter which does not change any more. Indeed all the coupling constants as defined in (4.8) are independent of momentum transfer or impact parameter. Any deviation of any given mode from the 4D shock wave form comes only by courtesy of its mass.

In the $L \ll \ell$ limit, the equation (4.31) should be understood as a perturbative result, obtained by the resummation of all the contributions to the shock wave profile that retain the *same* functional form in χ , namely those $\propto Q_1(\cosh \chi)$. These corrections communicate to the graviton the presence of the IR cutoff set by the AdS_4 curvature radius $1/\ell$: in locally localized gravity, the RS2 expression for M_4 receives higher order IR corrections whose leading terms found by expanding (4.31) are

$$M_4^2 = M_5^3 L \left(1 + \frac{5}{12} \left(\frac{L}{\ell}\right)^2 + \dots\right). \quad (4.32)$$

Further corrections can be easily extracted from (4.31). Such terms may provide for useful explicit checks of the dual CFT description.

Note that although the heavier gravitons have decoupled, the small graviton mass still yields a very weak distance running of G_{eff} , still defined – following (4.28) – as the coefficient of Q_1 in (4.30). However in this regime, the discrete slow jumping that dominated the changing of G_{eff} previously is replaced by a very slow continuous spatial variation, gently weakening gravity according to $\left(1 - \mathcal{O}(1) \frac{L^2}{\ell^2} \frac{\mathcal{R}}{\ell}\right)$. These corrections remain tiny until \mathcal{R} reaches ℓ^3/L^2 .

4.1.5 A Peek into AdS_5

Once we go to distances $\mathcal{R} > \ell^3/L^2$, the corrections from the ultralight graviton mass start altering the shock wave more significantly. Indeed from the asymptotics of the ultralight mode (4.21) we see that the shock wave (4.4) approaches

$$f(0, \chi \gg 1) = \frac{4}{3} \frac{p}{\pi M_4^2} e^{-(2+m^2\ell^2/3)\mathcal{R}/\ell}, \quad (4.33)$$

where we use $g_1^2 = 1/M_4^2$ of Eq. (4.31). Comparing this to the leading large distance behavior of the $4D$ GR shock wave on AdS_4 (4.2),

$$f_{4D\,AdS}(0, \chi \gg 1) = \frac{4}{3} \frac{p}{\pi M_4^2} e^{-2\mathcal{R}/\ell}. \quad (4.34)$$

we note the *extra* factor $\exp(-\frac{m^2\ell^2}{3}\frac{\mathcal{R}}{\ell})$. It arises from the interplay of the small mass and AdS_4 curvature, noted in Eqs. (4.16), (4.17). So if we compare it with the $4D$ form (4.34), extracting $G_{eff} = f/f_{\text{standard}}$ as before, we find

$$G_{eff} \simeq \frac{1}{M_2^4} e^{-(m^2\ell^2/3)\mathcal{R}/\ell}. \quad (4.35)$$

Thus probing the shock with deflections of probes very far away would suggest that the effective gravitational coupling continues to run, with distance along the brane, eventually going to zero at infinity. In the bulk this appears as a purely classical effect.

This scale dependence opens a small window into the fifth dimension. To see it, we compare (4.33) with the large radius behavior of the solutions of a Klein-Gordon equation with a small mass in AdS_{d+1} . That is sufficient because, due to Lorentz contraction, the shock wave profile in $d+1$ dimensions behaves like the gravitational potential of a source at rest in d dimensions. To find the scaling it is enough to consider large distance limit of solutions of a massive Klein-Gordon in AdS_{d+1} Poincare patch, given by the metric $ds_{AdS_{d+1}}^2 = \frac{r^2}{\ell^2}(d\vec{x}_{d-1}^2 - dt^2) + \frac{\ell^2}{r^2}dr^2$, and ignore the \vec{x}, t dependence, so that the massive Klein-Gordon equation reduces to⁷ $\left[\frac{r^2}{\ell^2}\partial_r^2 + (d+1)\frac{r}{\ell^2}\partial_r - m^2\right]\Phi = 0$. Its regular solution at infinity scales as $r^{-d-m^2\ell^2/d}$ for $m\ell \ll 1$. In terms of the physical distance $\mathcal{R} = \ell \log(r/\ell)$, this yields

$$\Phi_d \simeq e^{-(d+m^2\ell^2/d)\mathcal{R}/\ell}. \quad (4.36)$$

The lesson is that both the leading and the subleading decay rates of Φ are controlled by the *same* number d , counting the spatial dimensions of AdS .

⁷For exact expressions for scalar propagators in AdS , see [45] and references therein.

In contrast we see that in $AdS_4 \subset AdS_5$ framework, the shock wave is a hybrid:

$$f \simeq e^{-(2+m^2\ell^2/3)\mathcal{R}/\ell}. \quad (4.37)$$

The leading order decay rate is controlled by AdS_4 asymptotics, and is the same as for conventional massless GR in AdS_4 . The subleading order probes the full AdS_5 geometry, making long range gravitational force *weaker* than in $4D GR$ on AdS_4 . However it does so a bit more *slowly* than a perturbative graviton mass term would have done in AdS_4 alone, where as we have seen above the subleading correction to the decay rate would have been $\propto \exp[-(m^2\ell^2/2)\mathcal{R}/\ell]$. In other words, the rate of G_{eff} running discerns the influence of asymptotic AdS_5 . Note that this scaling is very similar with the scaling of the operator which acquires anomalous dimension in the dual CFT , which is responsible for the emergence of the graviton mass [20].

4.2 Recovering Minkowski

As we have already seen from (4.3), the shock wave (3.14) reduces in the leading order to the Aichelburg-Sexl solution at distances $L \ll \mathcal{R} \ll \ell$. The limit to RS2 corresponds to fixing L and taking $\ell \rightarrow \infty$. We also need to rescale $\chi = \mathcal{R}/\ell$ and keep \mathcal{R} fixed while sending ℓ to infinity. In this case the background (2.1) reduces to RS2, and so the Ansatz for the shock wave metric (2.6) goes to the form obtained by boosting a mass confined to the RS2 brane [36]. Our shock wave profile also reduces precisely to Emparan's solution as well. Of course, this is expected because of the symmetries of the theory and the limiting form of the masses and couplings (see Appendix C), which ensure that the spectrum reduces back to the RS2 one. Here we outline this limit, leaving more details for Appendix D.

We start with (4.22) and separate the ultralight mode $\propto g_1^2$ from the rest. When $\ell \rightarrow \infty$, the coupling reduces to the RS2 value $\frac{1}{M_5^3 L} = \frac{1}{M_4^2}$ and the mode function $Q_{\nu_1}(\chi)$ becomes exactly $Q_{\nu_1}(\cosh \chi) \rightarrow -\log(\mathcal{R}/2\ell) - 1$ because the higher order terms in (4.14) are proportional to $\mathcal{O}((\mathcal{R}/\ell)^2)$ and so they vanish when $\ell \rightarrow \infty$, while $\psi(2)+\gamma_E = 1$. Further, we can replace the normalization factor $1/\ell$ in the logarithm by $1/L$ by using a $4D$ diffeomorphism along the brane [28]. Thus the ultralight mode contribution yields

$$f_{A-S} = \frac{p}{\pi M_4^2} \log \frac{\mathcal{R}}{2L} + \frac{p}{\pi M_4^2}. \quad (4.38)$$

The sum of the massive modes reduces to an integral, thanks to properties of hypergeometric functions (see Appendix D.),

$$-\frac{p}{\pi} \lim_{\ell \rightarrow \infty, \mathcal{R} < \ell} \sum_{n=2}^{\infty} g_n^2 Q_{\nu_n}(\chi) = -\frac{p}{2\pi M_5^3 L} \int_0^{\infty} \frac{dm}{m} \frac{4}{\pi^2} \frac{K_0(m\mathcal{R})}{J_1(mL)^2 + Y_1(mL)^2}. \quad (4.39)$$

Adding (4.38) and (4.39) we obtain the RS2 shock wave on the brane found by Emparan [36] (where we use slightly different normalizations):

$$f_{RS2} = \frac{p}{\pi M_4^2} \log \frac{\mathcal{R}}{2L} + \frac{p}{\pi M_4^2} - \frac{p}{2\pi M_5^3 L} \int_0^\infty \frac{dm}{m} \frac{4}{\pi^2} \frac{K_0(m\mathcal{R})}{J_1(mL)^2 + Y_1(mL)^2}. \quad (4.40)$$

This is another nice check of the calculation.

It is instructive to scrutinize this limit more closely. Expanding the integrand in powers of mL we get

$$f_{RS2} = \frac{p}{\pi M_4^2} \log \frac{\mathcal{R}}{2L} + \frac{p}{\pi M_4^2} - \frac{p}{2\pi M_4^2} \frac{L^2}{\mathcal{R}^2} + \dots, \quad (4.41)$$

where we only keep the leading correction $\mathcal{O}(L^2/\mathcal{R}^2)$. This is the surviving correction from the intermediate gravitons in the limit $\ell \rightarrow \infty$. To see this, observe that in the limit $\ell \rightarrow \infty$ we can replace the sums in (4.27) with

$$\sum_{n=2}^{m < 2/\mathcal{R}} \rightarrow \int_{1/\ell}^{2/\mathcal{R}} \ell dm. \quad (4.42)$$

We regulate all mass integrals in the IR by the cutoff $\mu = 1/\ell$ since we only work in the box $\mathcal{R} < \ell$. This properly encodes the asymptotic behavior of the intermediate mass modes Q_{ν_n} . Using (4.13) as $\ell \rightarrow \infty$, the correction terms in (4.27) become

$$\begin{aligned} \mathcal{C} &= \frac{p}{\pi} \left(g_1^2 [\psi(\nu_1 + 1) + \gamma_E] + \sum_{n=2}^{m_{max} < 2/\mathcal{R}} g_n^2 [\psi(\nu_n + 1) + \gamma_E] \right) = \\ &= \frac{p}{\pi M_4^2} \left(1 + \frac{1}{2} \int_{1/\ell}^{2/\mathcal{R}} L^2 m dm \ln(\ell m) \right), \end{aligned} \quad (4.43)$$

where we have used $\psi(\nu_n + 1) + \gamma_E = \sum_{k=1}^n 1/k = \int_{1/\ell}^m \frac{dm}{m} = \ln(\ell m)$. Direct integration yields

$$\mathcal{C} = \frac{p}{\pi M_4^2} \left(1 - \frac{L^2}{\mathcal{R}^2} \ln\left(\frac{\mathcal{R}}{2\ell}\right) - \frac{1}{2} \frac{L^2}{\mathcal{R}^2} + \dots \right), \quad (4.44)$$

where we omit all the terms which vanish in the limit $\ell \rightarrow \infty$. We note that the second term has logarithmic divergences in the IR. On the other hand, we also find that Eq. (4.28) in this limit reduces to

$$G_{eff} = g_1^2 \left(1 + \frac{1}{2} \int_{1/\ell}^{2/\mathcal{R}} dm m L^2 + \dots \right) = \frac{1}{M_4^2} \left(1 + \frac{L^2}{\mathcal{R}^2} + \dots \right), \quad (4.45)$$

again ignoring all the terms $\propto L/\ell$ that vanish as $\ell \rightarrow \infty$. Plugging (4.44), (4.45) back into (4.27), we see that the $G_{eff} \ln(\mathcal{R}/2\ell)$ contains another logarithmic divergence

$\propto \frac{L^2}{\mathcal{R}^2} \ln(\frac{\mathcal{R}}{2\ell})$, but of opposite sign. Thus the logarithmic divergences cancel exactly, including the finite logarithmic pieces, and the surviving form of the shock is precisely the long distance limit of the RS2 shock (4.41), including the correct coefficients of all the leading terms.

This confirms our interpretation of slow jumpy changes in G_{eff} as a running induced by the CFT loops in the dual theory. Indeed we see that in the RS2 limit, the running precisely cancels the IR divergence coming from the IR contributions of the lightest CFT excitations, and the surviving subleading term in the shock wave solution at long distances is the finite CFT correction.

5. Conclusions

The bulk picture painted with our shock waves gives us glimpses of the dual AdS/CFT interpretation of locally localized gravity in terms of a defect CFT [11, 20]. Imagine that a fat defect, of size L and codimension one, has been built out of $4D$ CFT degrees of freedom, as proposed in [11, 20]. On the defect, the CFT is cut off in the UV at $1/L$, set by the thickness of the defect. If the defect is stable, or at least very long lived, its low energy excitations will be non-destructive because they correspond to a change of the internal structure of the defect. They are described by an effective field theory emerging from the dual CFT mixing with the defect [20]. The conformal symmetry of these excitations is broken down to a $SO(3, 2)$ subgroup at a low scale $1/\ell$, generated by the strong coupling dynamics. This scale at the moment is not calculable in a precise way, however there are compelling arguments pointing out how it can emerge in several different ways [20]. The discrete tower of intermediate bulk gravitons with masses $m \sim n/\ell < 1/L$ corresponds to the defect excitations, and their dynamics has been described by an effective CFT in AdS_4 [19]. The heavy gravitons with masses above $1/L$ are not a part of the CFT dual, but only emerge after we specify a UV completion of the cutoff, and in the case we consider they follow from the assumption that the bulk picture can be used all the way up to the $5D$ Planck scale M_5 .

After we impose the UV cutoff $1/L$, the local geometry around the defect becomes dynamical, described by $4D$ gravity whose Planck mass arises from the finite UV cutoff. Once the defect excitations and the IR cutoff ℓ are included, there will be additional terms in the vacuum polarization amplitude of the graviton, as argued in [11, 19, 20], which will also receive contributions which depend on the external momentum, on the masses of the CFT excitations and on the IR cutoff $1/\ell$. In the effective CFT on AdS_4 picture, these latter terms will come, for example, from the lower limit of momentum integration over the defect excitations in the loops. In this description of the defect dynamics, the new terms influence the graviton dynamics in several different ways. The

corrections from the IR cutoff, by conformal symmetry, will yield a correction to the graviton 2-point function, scaling as $1/\ell^4$, which is weighed by the two powers of the graviton coupling $1/M_4$ and multiplied by the number of *CFT* degrees of freedom. This gives $m^2 \sim g_* \frac{1}{M_4^2} \frac{1}{\ell^4} \sim \frac{L^2}{\ell^4}$, exactly the ultralight graviton mass [19]. In the defect *CFT* this is interpreted as the statement that some operator acquires a small anomalous dimension in the presence of the defect [20]. Further these terms will also correct the formula for the 4D Planck scale, defined as the coupling of the ultralight mode, which should really be $M_4^2 \sim g_*/L^2(1 + O(L^2/\ell^2))$, where $g_* = M_5^3 L^3$ is the number of *CFT* degrees of freedom and $O(L^2/\ell^2)$ are the higher order quantum corrections from the defect excitations deformed at the IR cutoff ℓ . Indeed from our exact shock wave calculation (1.1) we find that $M_4^2 = M_5^3 L \left(1 + \frac{5}{12}(\frac{L}{\ell})^2 + \dots\right)$, in agreement with the estimate based on effective field theory.

The corrections which depend on the external momentum and masses of defect excitations are again in agreement with the description of the defect by an effective *CFT* in AdS_4 [19]. The defect excitations in the graviton vacuum polarization diagrams renormalize the Newton's constant G_{eff} , dressing up the coupling and making the graviton look composite at distances below ℓ . We have seen how this works explicitly by taking the limit of $\ell \rightarrow \infty$, where we restore the RS2 shock wave found by Emparan [36], where the excitation-induced running of G_{eff} precisely cancels the logarithmic singularities in the subleading long range contributions from the intermediate modes, and renders the shock finite. The surviving terms are precisely the remaining *CFT* vacuum polarization corrections to the graviton at large distances.

Because of the details of the embedding of the AdS_4 brane in the bulk, from the bulk point of view our relativistic projectile moves along a trajectory which is *not* a null geodesic in the full bulk. Since the particle is stuck on the brane, there is a force induced by the brane's structure which acts on it, and so its trajectory is deformed away from a bulk null geodesic. From the dual *CFT* point of view, a shock wave of a null particle in the bulk is interpreted as an excitation of the light cone states of the dual *CFT* [35]. Hence the shock wave of a source on the brane should correspond to the light cone states “fattened” by the interactions with the defect. Far from the source the defect excitations decouple because of the gap in their spectrum, and the only signature of the defect is the small mass of the ultralight graviton, which drives the shock field to zero faster than in 4D *GR* (but more slowly than a perturbative graviton mass term would have done in AdS_4). If we extract the effective Newton's constant far from the source by comparison with the solution in AdS_4 , we see that it goes to zero as a function of distance at a rate set by the anomalous dimension of the operator which should be dual to the graviton in $AdS_4 \subset AdS_5$. This points to a

connection with the holographic rescaling in the boundary *CFT* [27], and it would be interesting to explore further. Note that the most dramatic deviations from the $4D$ become noticeable through the subleading corrections to the shock wave profile only at distances $\mathcal{R} > \ell^3/L^2$ along the brane.

In sum, in this paper we have presented the exact solution for the gravitational field of a relativistic particle living on an AdS_4 brane in AdS_5 space. The solution is the first exact background in the framework of locally localized gravity in AdS braneworlds. As advocated in [37] the shock wave is a powerful tool for investigating the nature of the transverse traceless graviton sector. From exploring the solution we find the precise formula for the $4D$ Planck mass relating it to the $5D$ Planck mass and the curvature radii. It includes higher order corrections that depend on the AdS_4 radius ℓ , and reduces to the RS2 expression as $\ell \rightarrow \infty$. In the dual *CFT* description, this is interpreted as corrections from the IR, where strong coupling effects in the defect *CFT* manufacture the IR scale $1/\ell$. This is also consistent with holographic arguments suggested in [18], who noted that the dual description of the $AdS_4 \subset AdS_5$ system can only cover a portion of the bulk AdS_5 space transverse to the AdS_4 brane. Our shock gives an interesting explicit handle for exploring these IR modifications in the dual *CFT*. We also confirm that the shock wave looks $5D$ at short distances and approximates very closely the $4D$ AdS shock wave in the leading order. However at distances $\mathcal{R} \gtrsim \ell^3/L^2$ along the brane, the subleading terms become important because they induce an extra correction to the decay rate of the graviton wave function along the brane. The correction knows of the presence of the extra dimension, and leads to subleading deviations from the AdS_4 shock wave of [34], which a $4D$ observer may interpret as a spatial “running” of the $4D$ effective gravitational coupling. Following this variation of G_{eff} at large \mathcal{R} one would be able to count up all spatial dimensions without ever moving away from the brane. In [18] the authors offer a qualitative argument based on light-sheet holography, suggesting that gravity may remain $4D$ all the way out to infinity if it is probed over times shorter than ℓ . We find a somewhat stronger version of this statement, which is that gravity deviates away from $4D$ *GR* in a significant way only at distances $\gtrsim \ell^3/L^2$ along the brane.

In our solution the scalar graviton mode, present whenever there is a mass term [17], is conspicuously missing. The reason is the same as the one encountered in the construction of shock waves in DGP braneworlds [37]. Relativistic perturbations on the brane have a vanishing stress-energy tensor trace, $T^\mu{}_\mu = 0$, and therefore do not source the scalar graviton field. This logic is consistent barring the problems with strong coupling, which may be under control here thanks to the perturbation theory results of [14, 15, 16]. One may be able to test this explicitly by considering very fast particles with non-zero rest mass, moving with a speed $v \rightarrow c$ as sources, and including the effect

of their mass. They would source the scalar graviton, which should be a perturbation on top of the shock wave, suppressed by the source mass-to-momentum ratio $M/p = \sqrt{1/v^2 - 1} \ll 1$ [37]. It would be interesting to investigate the perturbative dynamics of the scalar and its implications for locally localized gravity and for its dual description in more detail.

Acknowledgments

We thank Thibault Damour, Roberto Emparan, Ted Jacobson, Andreas Karch, Konstadinos Sfetsos and John Terning for useful discussions. N.K. is grateful to IHES, Bures-sur-Yvette, France, for kind hospitality during this work. L.S. acknowledges the kind hospitality of the Theory Division, CERN, during the course of this work. This work was supported in part by the DOE Grant DE-FG03-91ER40674, in part by the NSF Grant PHY-0332258 and in part by a Research Innovation Award from the Research Corporation.

A. Derivation of the Wave Profile Field Equation

To evaluate G_{5B}^A in (2.7) we can use the same conformal transformation trick as in [37], splitting the metric as $ds^2 = \Omega^2 d\bar{s}^2$, where

$$d\bar{s}^2 = \frac{4 du dv}{(1 - uv/\ell^2)^2} - \frac{4\delta(u)f du^2}{(1 - uv/\ell^2)^2} + \ell^2 \left(\frac{1 + uv/\ell^2}{1 - uv/\ell^2} \right)^2 (d\chi^2 + \sinh^2 \chi d\phi^2) + dz^2. \quad (\text{A.1})$$

We could now proceed with a straightforward albeit tedious computation of the Einstein tensor for $d\bar{s}^2$, treating $\delta(u)$ and its derivatives as distributions. We can shorten the labor, however, by noting that the metric (A.1) is related to the conformal de Sitter metric, Eq. (12) of the second of references [37], by a substitution

$$\frac{1}{\ell} = iH, \quad \chi = i\theta. \quad (\text{A.2})$$

Hence we can take the components of the Ricci tensor computed there and map them back, finding

$$\begin{aligned} \bar{R}_{5uu} &= 2\delta(u) \left(\partial_z^2 f + \frac{1}{\ell^2} (\Delta_2 f + 4f) \right), \\ \bar{R}_{5uv} &= -\frac{6}{\ell^2 (1 - uv/\ell^2)^2}, \\ \bar{R}_{5ab} &= -3 \left(\frac{1 + uv/\ell^2}{1 - uv/\ell^2} \right)^2 g_{ab}, \end{aligned} \quad (\text{A.3})$$

where \bar{R}_{5AB} is the Ricci tensors of (A.1) and a, b and g_{ab} are the indices and the metric on the “unit” \mathcal{H}_2 , respectively. The operator Δ_2 is the Laplacian on the “unit” \mathcal{H}_2 , where we have properly accounted for the sign flips from the map (A.2). Now we “invert” the conformal transformation $ds_5^2 = \Omega^2 d\bar{s}_5^2$ to find the Ricci tensor for ds^2 , given by

$$R_{5AB} = \bar{R}_{5AB} - 3\bar{\nabla}_A \bar{\nabla}_B \ln \Omega + 3\bar{\nabla}_A \ln \Omega \bar{\nabla}_B \Omega - \bar{g}_{AB} \left(\bar{\nabla}^2 \ln \Omega + 3(\bar{\nabla} \ln \Omega)^2 \right), \quad (\text{A.4})$$

which, with $\Omega(|z|) = \left[L / [\ell \sin(|z| + z_0)/\ell] \right]$, and using distributional rules for the derivatives of δ -functions, e.g. $u\delta(u) = 0$, $u^2\delta^2(u) = 0$ and $f(u)\delta'(u) = -f'(u)\delta(u)$ [28, 34], yields

$$\begin{aligned} R_{5zz} &= -4\partial_z \left(\frac{\partial_z \Omega}{\Omega} \right), \\ R_{5uu} &= 2\delta(u) \left(\partial_z^2 f + 3\frac{\partial_z \Omega}{\Omega} \partial_z f + \frac{1}{\ell^2} (\Delta_2 f - 2f) \right) + 4\partial_z \left(\frac{\partial_z \Omega}{\Omega} \right) f \delta(u), \\ R_{5uv} &= -\frac{2}{(1 - uv/\ell^2)^2} \partial_z \left(\frac{\partial_z \Omega}{\Omega} \right), \\ R_{5ab} &= \ell^2 \left(\frac{1 + uv/\ell^2}{1 - uv/\ell^2} \right)^2 g_{ab} \partial_z \left(\frac{\partial_z \Omega}{\Omega} \right). \end{aligned} \quad (\text{A.5})$$

From the definition of Ω , we have

$$\begin{aligned} \frac{\partial_z \Omega}{\Omega} &= -\frac{2\Theta(z) - 1}{\ell} \cot[(|z| + z_0)/\ell], \\ \partial_z \left(\frac{\partial_z \Omega}{\Omega} \right) &= -2\frac{\cot[(|z| + z_0)/\ell]}{\ell} \delta(z) + \frac{1}{\ell^2 \sin^2[(|z| + z_0)/\ell]}. \end{aligned} \quad (\text{A.6})$$

Clearly, in the presence of the shock wave the bulk is not AdS_5 any more, since the waves extend off the brane and deform the bulk. This can be seen from the last term of R_{5uu} , and also from the Riemann tensor. Now, we can rewrite (2.7) as

$$\begin{aligned} R_{5B}^A &= -\frac{4}{L^2} \delta^A_B + 2 \left(\frac{1}{L^2} - \frac{1}{\ell^2} \right)^{1/2} \delta(z) \left(4\delta^A_B - 3\delta^\mu_\nu \delta_\mu^A \delta_B^\nu \right) \\ &\quad + 2 \frac{p}{M_5^3 \ell^2} \frac{1}{\sinh \chi} \delta_v^\mu \delta_\nu^u \delta_\mu^A \delta_B^\nu \delta(\chi) \delta(\phi) \delta(u) \delta(z). \end{aligned} \quad (\text{A.7})$$

The new equation for the wave profile f comes from the uu component of (A.7). Using $\delta(\chi)/\sinh \chi = \delta(\cosh \chi - 1)$, after a straightforward calculation we find that the linear field equation for the wave profile is

$$\partial_z^2 f + 3\frac{\partial_z \Omega}{\Omega} \partial_z f + \frac{1}{\ell^2} (\Delta_2 f - 2f) = \frac{2p}{M_5^3 \ell^2} \delta(\cosh \chi - 1) \delta(\phi) \delta(z) \quad (\text{A.8})$$

The remaining components of (A.7) are trivially satisfied by virtue of the background equation $L/\ell = \sin(z_0/\ell)$.

We note that in the case of *AdS* backgrounds the procedures to solve this equation are more straightforward (albeit technically more involved) than in de Sitter background. The reason is that the space transverse to the source of the shock wave is non-compact, and so implementing the boundary conditions for the single particle problem is simpler, as there do not arise additional singularities that appear on a 2-sphere in de Sitter [32, 33, 34].

B. Series Representation of the Shock Wave

Here we derive the series representation of the shock wave, Eq. (4.4) from the integral formula (3.14). Using Eq. (3.3.1 (8)) of [42] we write

$$P_\nu(z) = \frac{\sin(\pi\nu)}{\pi \cos(\pi\nu)} [Q_\nu(z) - Q_{-\nu-1}(z)] . \quad (\text{B.1})$$

After doubling up the domain of integration in (4.4) according to $\int_0^\infty = (1/2) \int_{-\infty}^\infty$, using (B.1) we rewrite it as

$$f(0, \chi) = \frac{p}{2\pi M_5^3 \ell} \frac{1}{2\pi i} \int_{-\infty}^\infty dq q \frac{P_{iq-1/2}^{-2}(-\cos(y_0))}{P_{iq-1/2}^{-1}(-\cos(y_0))} \times \\ \times [Q_{iq-1/2}(\cosh \chi) - Q_{-iq-1/2}(\cosh \chi)] . \quad (\text{B.2})$$

To evaluate the integral, we split it into two parts setting $f = f^+ + f^-$, where

$$f^+ = \frac{p}{2\pi M_5^3 \ell} \frac{1}{2\pi i} \int_{-\infty}^\infty dq q \frac{P_{iq-1/2}^{-2}(-\cos(y_0))}{P_{iq-1/2}^{-1}(-\cos(y_0))} Q_{iq-1/2}(\cosh \chi) , \\ f^- = \frac{p}{2\pi M_5^3 \ell} \frac{i}{2\pi} \int_{-\infty}^\infty dq q \frac{P_{iq-1/2}^{-2}(-\cos(y_0))}{P_{iq-1/2}^{-1}(-\cos(y_0))} Q_{-iq-1/2}(\cosh \chi) . \quad (\text{B.3})$$

Notice that by the reality of the Legendre functions, the two integrals f^\pm are complex conjugates of each other, if they are convergent: $f^- = (f^+)^*$. Thus to evaluate f , it is sufficient to only compute one of f^\pm . Let us compute f^+ . For large q , the integrand of this integral goes as $\exp(-iq\chi)$ (see [43], Eq. (8.723.2)). Therefore we can close the integration contour on the half q -plane where $\text{Im}[q] < 0$. Defining $\nu \equiv iq - 1/2$, the integration yields

$$f^+ = \frac{p}{4\pi M_5^3 \ell} \sum_{\nu > -1/2} (2\nu + 1) \frac{P_\nu^{-2}(-\cos(y_0))}{\partial_\nu P_\nu^{-1}(-\cos(y_0))} Q_\nu(\cosh \chi) . \quad (\text{B.4})$$

where the sum runs over all the poles of the integrand, located at the values of $\nu > -1/2$ for which $P_\nu^{-1}(-\cos(y_0)) = 0$. Because f^+ is finite (except for the short distance singularities, of course) and real, $f^- = f^+$, and hence $f = 2f^+$, or

$$f(0, \chi) = \frac{p}{2\pi M_5^3 \ell} \sum_{\nu > -1/2} (2\nu + 1) \frac{P_\nu^{-2}(-\cos(y_0))}{\partial_\nu P_\nu^{-1}(-\cos(y_0))} Q_\nu(\cosh \chi), \quad \nu = iq - 1/2. \quad (\text{B.5})$$

C. Spectrum of $AdS_4 \subset AdS_5$: Masses and Couplings

Here we determine the masses and couplings of graviton modes in the limit $L \ll \ell$. The modes are determined by the secular equation (4.5). A suitable expression for the Legendre function $P_\nu^{-1}(x)$ is

$$P_\nu^{-1}(x) = \left(\frac{1-x}{1+x} \right)^{1/2} F(-\nu, 1+\nu; 2; 1/2 - x/2), \quad (\text{C.1})$$

which means that the problem of finding the eigenmodes reduces to finding the roots of the hypergeometric function. In the small $y_0 = L/\ell + \dots$ limit, we substitute $x = -\cos(y_0) \simeq -1 + y_0^2/2$ in the hypergeometric function and expand it. The series representation is

$$\frac{1}{\Gamma(2+\nu)\Gamma(1-\nu)} \left\{ 1 + \nu(\nu+1) \frac{y_0^2}{4} \sum_{j=0}^{\infty} \frac{(2+\nu)_j (1-\nu)_j}{(j+1)! j!} \left[h_j - \log \frac{y_0^2}{4} \right] \left(\frac{y_0^2}{4} \right)^j \right\}, \quad (\text{C.2})$$

where

$$h_j = \psi(1+j) + \psi(2+j) - \psi(2+\nu+j) - \psi(1-\nu+j), \quad (\text{C.3})$$

and $\psi(z)$ is the logarithmic derivative of the Γ -function. We only consider the leading order expressions for the masses, and so in the small y_0 limit, we can truncate the series (C.2) to the leading order in y_0 , which means drop all the terms beyond $j=0$. In this limit the secular equation reduces to

$$\nu(\nu+1) [\psi(2+\nu) + \psi(1-\nu) - \psi(1) - \psi(2)] = \frac{4}{y_0^2} + \nu(\nu+1) \log \frac{y_0^2}{4}. \quad (\text{C.4})$$

Further, in this limit we can ignore the logarithm on the RHS for intermediate graviton modes $|\nu| < 1/y_0$. By analyticity of the integration that produced the series representation of the shock wave (B.5), we must require $\nu > -1/2$. Then the large contribution from y_0 , which grows as a second order pole, can be compensated by the singularities

of the ψ function, which has poles at negative integers and zero. Given the constraint $\nu > -1/2$, we see that the only relevant term on the LHS is $\psi(1-\nu)$. So whenever ν approaches a positive integer, ψ shoots up sufficiently quickly to match the $1/y_0^2$ term. Setting $\nu = n + \varepsilon$ with $n = 1, 2, 3, \dots$ and a small ε , we find $\psi(1-n-\varepsilon) = 1/\varepsilon + \text{finite terms}$. Substituting this in (C.4), we can solve for ε , or equivalently for ν_n , to the leading order in $y_0 = L/\ell + \dots$. We find

$$\nu_n = n + \frac{y_0^2}{4} n(n+1) + \dots, \quad n = 1, 2, 3, \dots \quad (\text{C.5})$$

The masses of the spectrum, by $m^2 = \frac{\nu(\nu+1)-2}{\ell^2}$, are therefore given by

$$m^2 = \frac{1}{\ell^2} \left[(n-1)(n+2) + \frac{1}{2} n(n+1/2)(n+1) \frac{L^2}{\ell^2} \right] + \dots, \quad n = 1, 2, 3, \dots \quad (\text{C.6})$$

When $\varepsilon \sim n^2 y_0^2/4$ ceases to be small, for $n \sim 2/y_0$, the above formula for the KK masses should be replaced. This happens when the mass reaches $m \sim 1/L$. At such high scales, effects of the curvature can be ignored, and the system behaves effectively as a box of size $2(\pi - y_0)\ell$. Starting with the expansion valid for large ν

$$P_\nu^\mu(-\cos y_0) \simeq \frac{\Gamma(\nu + \mu + 1)}{\Gamma(\nu + 3/2)} \left(\frac{2}{\pi \sin y_0} \right)^{1/2} \cos \left[\left(\nu + \frac{1}{2} \right) (\pi - y_0) + \frac{2\mu - 1}{4} \pi \right], \quad (\text{C.7})$$

in the secular equation (C.6) we find that the eigenvalues in this regime are

$$\nu_n = -\frac{1}{2} + \frac{\pi/4 + n\pi}{\pi - y_0} + \dots = n(1 + y_0/\pi) + \dots, \quad n \gtrsim 2/y_0. \quad (\text{C.8})$$

Therefore the heavy graviton masses are

$$m^2 = \frac{1}{\ell^2} \left[n^2 + n + \frac{2L^2}{\pi\ell^2} n^2 \right] + \dots, \quad n \gtrsim \frac{\ell}{L}. \quad (\text{C.9})$$

Note that these modes are above the *CFT* cutoff $1/L$, and hence are not in the calculable regime of a dual *CFT*, but are still well defined on the bulk side as long as $L \ll 1/M_5$ (and de facto negligible at all but the shortest distances $\mathcal{R} < L$).

We now determine the couplings of these modes. From the series expression for the shock wave profile (4.4) we can simply read off the couplings as the coefficients of $Q_\nu(\cosh \chi)$:

$$g_n^2 = -\frac{2\nu + 1}{2M_5^3 \ell} \frac{P_\nu^{-2}(-\cos(y_0))}{\partial_\nu P_\nu^{-1}(-\cos(y_0))} \Big|_{\nu=\nu_n}. \quad (\text{C.10})$$

This formula is an exact bulk expression for couplings of each individual graviton mode to the matter on the brane. The (-) sign compensates the fact that $\partial_\nu P_\nu^{-1}(-\cos(y_0))$ is negative.

We next express the couplings as functions of the mode masses to the leading order in $y_0 \ll 1$. We determine $P_\nu^{-2}(-\cos(y_0))$ from (3.8) and $\partial_\nu P_\nu^{-1}(-\cos(y_0))$ using the leading-order truncation of (C.2). After a straightforward calculation this yields

$$g_n^2 = \frac{L}{4M_5^3 \ell^2} \frac{(2n+1)n(n+1)}{n+2} \frac{1}{n-1+n(n+1)(L^2/4\ell^2)}. \quad (\text{C.11})$$

Note that the coupling of the ultralight mode, $g_1 = \frac{1}{M_4^2}$ is *much* stronger than that of the other modes: it is

$$g_1^2 = \frac{1}{M_5^3 L} + \dots, \quad (\text{C.12})$$

i.e. just the standard RS2 Newton's constant, whereas the couplings of heavier modes are suppressed relative to it by powers of L/ℓ . In fact using (C.6) and omitting higher order terms we can rewrite the couplings of heavy modes as

$$g_m^2 \simeq \frac{mL}{2M_5^3 \ell} = \frac{1}{2M_4^2} \frac{L}{\ell} mL. \quad (\text{C.13})$$

As mass increases, this formula eventually saturates to $g_m^2 \simeq \frac{1}{M_5^3 \ell}$. This is reminiscent of the tunnelling suppression of bulk modes in RS2 [1, 23].

D. The Limit of RS2 Shock Wave

Here we outline how to take the RS2 limit $\ell \rightarrow \infty$ and recover the result of the shock wave calculation of [36]. Our starting point is the series representation (B.5) of the shock wave profile

$$f(0, \chi) = \frac{p}{2\pi M_5^3 \ell} \sum_{\nu > -1/2} (2\nu+1) \frac{P_\nu^{-2}(-\cos y_0)}{\partial_\nu P_\nu^{-1}(-\cos y_0)} Q_\nu(\cosh \chi), \quad (\text{D.1})$$

$$P_\nu^{-1}(-\cos y_0) = 0. \quad (\text{D.2})$$

First of all, we separate the ultralight mode contribution which reduces to (4.38) in the limit $\ell \rightarrow \infty$. That leaves the heavier modes.

Now, using the relation ([42], Eq. 3.4 (14))

$$P_\nu^\mu(-x) = P_\nu^\mu(x) \cos(\pi(\nu + \mu)) - (2/\pi) Q_\nu^\mu(x) \sin(\pi(\nu + \mu)) \quad (\text{D.3})$$

we rewrite the condition (D.2) as

$$\frac{\cos \pi \nu}{\sin \pi \nu} = \frac{2}{\pi} \frac{Q_\nu^{-1}(\cos y_0)}{P_\nu^{-1}(\cos y_0)}. \quad (\text{D.4})$$

From this and Eq. (D.3) we obtain

$$P_\nu^{-2}(-\cos y_0) = \frac{2}{\pi} \frac{\sin \pi \nu}{P_\nu^{-1}(\cos y_0)} [P_\nu^{-2}(\cos y_0) Q_\nu^{-1}(\cos y_0) - P_\nu^{-1}(\cos y_0) Q_\nu^{-2}(\cos y_0)] \quad (\text{D.5})$$

In a similar fashion, we rewrite (first using (D.3), and then using (D.4) having taken a derivative with respect to ν)

$$\begin{aligned} \partial_\nu P_\nu^{-1}(-\cos y_0) &= \frac{2}{\pi} \frac{\sin \pi \nu}{P_\nu^{-1}(\cos y_0)} \left\{ P_\nu^{-1}(\cos y_0) \left[\partial_\nu Q_\nu^{-1}(\cos y_0) + \frac{\pi^2}{2} P_\nu^{-1}(\cos y_0) \right] \right. \\ &\quad \left. + Q_\nu^{-1}(\cos y_0) [-\partial_\nu P_\nu^{-1}(\cos y_0) + 2 Q_\nu^{-1}(\cos y_0)] \right\} . \end{aligned} \quad (\text{D.6})$$

Thus we get

$$\frac{P_\nu^{-2}(-\cos y_0)}{\partial_\nu P_\nu^{-1}(-\cos y_0)} = \frac{P_\nu^{-2} Q_\nu^{-1} - P_\nu^{-1} Q_\nu^{-2}}{P_\nu^{-1} [\partial_\nu Q_\nu^{-1} + (\pi^2/2) P_\nu^{-1}] + Q_\nu^{-1} [-\partial_\nu P_\nu^{-1} + 2 Q_\nu^{-1}]} \quad (\text{D.7})$$

with all the functions at the right hand side evaluated at $+\cos y_0$.

Now we can go to the limit $\ell \rightarrow \infty$. In this limit, the masses are related to the values of ν by

$$m_n \simeq \nu_n/\ell \simeq n/\ell, \quad n = 1, 2, \dots, \quad (\text{D.8})$$

and m becomes a continuous index, so that we can replace \sum_n by $\int \ell dm$. Since $y_0 \simeq L/\ell$, $\nu \simeq m\ell$, $\chi = \mathcal{R}/\ell$ we can rewrite

$$\begin{aligned} P_\nu^\mu(\cos y_0) &= P_{m\ell}^\mu \left(\cos \frac{mL}{m\ell} \right), \quad Q_\nu^\mu(\cos y_0) = Q_{m\ell}^\mu \left(\cos \frac{mL}{m\ell} \right), \\ Q_\nu(\cosh \chi) &= Q_{m\ell} \left(\cosh \frac{m\mathcal{R}}{m\ell} \right). \end{aligned} \quad (\text{D.9})$$

Then we send ℓ to infinity while keeping m , L , \mathcal{R} finite, and use the relations ([44], Eqs. 9.1.71 & 72; 9.6.49 & 50), valid in the limit $\sigma \rightarrow \infty$

$$\begin{aligned} \sigma^\mu P_\sigma^{-\mu} \left(\cos \frac{x}{\sigma} \right) &\rightarrow J_\mu(x) & \sigma^\mu Q_\sigma^{-\mu} \left(\cos \frac{x}{\sigma} \right) &\rightarrow -\frac{\pi}{2} Y_\mu(x) \\ \sigma^\mu P_\sigma^{-\mu} \left(\cosh \frac{x}{\sigma} \right) &\rightarrow I_\mu(x) & \sigma^\mu Q_\sigma^{-\mu} \left(\cosh \frac{x}{\sigma} \right) &\rightarrow e^{i\mu\pi} K_\mu(x) \end{aligned} \quad (\text{D.10})$$

Our sum over massive modes then converges to the integral

$$\frac{p}{2\pi M_5^3} \int dm \frac{2}{\pi} K_0(m\mathcal{R}) \frac{J_1(mL) Y_2(mL) - Y_1(mL) J_2(mL)}{J_1(mL)^2 + Y_1(mL)^2} \quad (\text{D.11})$$

where we have used the fact that the terms of the form $\partial_\nu P_\nu^\mu$, $\partial_\nu Q_\nu^\mu$, give results that are proportional to L/ℓ and thus vanish in the Minkowski limit.

Finally, we use the Wronskian relation ([44], Eq. 9.1.16)

$$J_{\nu+1}(z) Y_{\nu}(z) - Y_{\nu+1}(z) J_{\nu}(z) = \frac{2}{\pi z}, \quad (\text{D.12})$$

to simplify (D.11). Including the ultralight mode contribution in this limit, we finally find

$$f(\chi, 0)|_{\ell \rightarrow \infty} = \frac{p}{\pi M_s^3 L} \left[\log \frac{\mathcal{R}}{2L} + 1 - \frac{1}{2} \int \frac{dm}{m} \frac{4}{\pi^2} \frac{K_0(m\mathcal{R})}{J_1(mL)^2 + Y_1(mL)^2} \right] \quad (\text{D.13})$$

which agrees with the result (16) of [36], once we account for a change in overall normalization.

References

- [1] L. Randall and R. Sundrum, Phys. Rev. Lett. **83** (1999) 4690.
- [2] N. Arkani-Hamed, S. Dimopoulos, G. R. Dvali and N. Kaloper, Phys. Rev. Lett. **84** (2000) 586.
- [3] N. Kaloper, JHEP **0405** (2004) 061.
- [4] N. Kaloper, Phys. Rev. D **60** (1999) 123506.
- [5] J. M. Maldacena, Adv. Theor. Math. Phys. **2** (1998) 231; S. S. Gubser, I. R. Klebanov and A. M. Polyakov, Phys. Lett. B **428** (1998) 105; E. Witten, Adv. Theor. Math. Phys. **2** (1998) 253; for a review see O. Aharony, S. S. Gubser, J. M. Maldacena, H. Ooguri and Y. Oz, Phys. Rept. **323** (2000) 183.
- [6] J. Maldacena, unpublished; E. Witten, unpublished; H. Verlinde, Nucl. Phys. B **580** (2000) 264; S. S. Gubser, Phys. Rev. D **63** (2001) 084017; S. B. Giddings, E. Katz and L. Randall, JHEP **0003** (2000) 023; M. J. Duff and J. T. Liu, Phys. Rev. Lett. **85** (2000) 2052 [Class. Quant. Grav. **18** (2001) 3207]; N. Arkani-Hamed, M. Porrati and L. Randall, JHEP **0108** (2001) 017.
- [7] O. DeWolfe, D. Z. Freedman, S. S. Gubser and A. Karch, Phys. Rev. D **62** (2000) 046008.
- [8] A. Karch and L. Randall, JHEP **0105**, 008 (2001)
- [9] A. Miemiec, Fortsch. Phys. **49** (2001) 747; M. D. Schwartz, Phys. Lett. B **502** (2001) 223.
- [10] A. Karch and L. Randall, Phys. Rev. Lett. **87**, 061601 (2001)

- [11] A. Karch and L. Randall, JHEP **0106**, 063 (2001)
- [12] H. van Dam and M. J. G. Veltman, Nucl. Phys. B **22** (1970) 397; V. I. Zakharov, JETP Lett. **12** (1970) 312.
- [13] A. I. Vainshtein Phys. Lett. B **39** (1972) 393.
- [14] I. I. Kogan, S. Mouslopoulos and A. Papazoglou, Phys. Lett. B **503** (2001) 173; Phys. Lett. B **501**, 140 (2001)
- [15] A. Karch, E. Katz and L. Randall, JHEP **0112**, 016 (2001)
- [16] N. Arkani-Hamed, H. Georgi and M. D. Schwartz, Annals Phys. **305** (2003) 96.
- [17] S. Deser and R. I. Nepomechie, Annals Phys. **154** (1984) 396; A. Higuchi, Nucl. Phys. B **282** (1987) 397.
- [18] R. Bousso and L. Randall, JHEP **0204** (2002) 057
- [19] M. Porrati, Phys. Rev. D **65** (2002) 044015; JHEP **0204** (2002) 058; Mod. Phys. Lett. A **18** (2003) 1793; M. J. Duff, J. T. Liu and H. Sati, Phys. Rev. D **69** (2004) 085012.
- [20] O. DeWolfe, D. Z. Freedman and H. Ooguri, Phys. Rev. D **66** (2002) 025009; O. Aharony, O. DeWolfe, D. Z. Freedman and A. Karch, JHEP **0307** (2003) 030.
- [21] F. A. E. Pirani, Proc. R. Soc. A **252** (1959) 96.
- [22] P. C. Aichelburg and R. U. Sexl, Gen. Rel. Grav. **2** (1971) 303.
- [23] S. Dimopoulos, S. Kachru, N. Kaloper, A. E. Lawrence and E. Silverstein, Phys. Rev. D **64** (2001) 121702; Int. J. Mod. Phys. A **19** (2004) 2657.
- [24] G. 't Hooft, Phys. Lett. B **198** (1987) 61.
- [25] D. Amati, M. Ciafaloni and G. Veneziano, Phys. Lett. B **197** (1987) 81; Int. J. Mod. Phys. A **3** (1988) 1615; I. J. Muzinich and M. Soldate, Phys. Rev. D **37** (1988) 359.
- [26] N. Arkani-Hamed, S. Dimopoulos and G. R. Dvali, Phys. Lett. B **429** (1998) 263; Phys. Rev. D **59** (1999) 086004.
- [27] L. Susskind and E. Witten, arXiv:hep-th/9805114.
- [28] T. Dray and G. 't Hooft, Nucl. Phys. B **253** (1985) 173; Class. Quant. Grav. **3** (1986) 825.
- [29] V. Ferrari, P. Pendenza and G. Veneziano, Gen. Rel. Grav. **20** (1988) 1185.
- [30] H. de Vega and N. Sanchez, Nucl. Ph. B **317** (1989) 706.

- [31] C. Barrabes and P. A. Hogan, Phys. Rev. D **64** (2001) 044022.
- [32] M. Hotta and M. Tanaka, Class. Q. Grav. **10** (1993) 307.
- [33] J. Podolsky and J. Griffiths, Phys. Rev. D **56** (1997) 4756.
- [34] K. Sfetsos, Nucl. Phys. B **436** (1995) 721.
- [35] G. T. Horowitz and N. Itzhaki, JHEP **9902** (1999) 010.
- [36] R. Emparan, Phys. Rev. D **64** (2001) 024025.
- [37] N. Kaloper, Phys. Rev. Lett. **94** (2005) 181601; Phys. Rev. D **71** (2005) 086003
[Erratum-ibid: **D71** (2005) 086003].
- [38] K. Sfetsos, Phys. Rev. D **52** (1995) 2323; arXiv:hep-th/0507134.
- [39] G. R. Dvali, G. Gabadadze and M. Porrati, Phys. Lett. B **485** (2000) 208; G. R. Dvali
and G. Gabadadze, Phys. Rev. D **63** (2001) 065007.
- [40] M. Bander and C. Itzykson, Rev. Mod. Phys. **38** (1966) 346.
- [41] C. Grosche and F. Steiner, Annals Phys. **182** (1988) 120.
- [42] *Bateman Manuscript Project: Higher Transcendental Functions*, ed. A Erdelyi,
McGraw-Hill, New York, 1953.
- [43] I. S. Gradshteyn and I. M. Ryzhik, *Table of Integrals, Series and Products*, Academic
Press, New York, 1980.
- [44] M. Abramowitz and I. A. Stegun, *Handbook of Mathematical Functions*, Dover
Publications, 1974.
- [45] E. D'Hoker and D. Z. Freedman, Nucl. Phys. B **550** (1999) 261.